THE ASTROPHYSICAL JOURNAL, 405:522–537, 1993 March 10

NEAR-INFRARED LINE IMAGING OF NGC 6240: COLLISION SHOCK AND NUCLEAR STARBURST

PAUL P. VAN DER WERF, R. GENZEL, A. KRABBE, M. BLIETZ, D. LUTZ, AND S. DRAPATZ
Max-Planck-Institut für Extraterrestrische Physik, Giessenbachstraße, D-8046 Garching bei München, Germany
MARTIN J. WARD
Oxford University, Department of Astrophysics, Keble Road, Oxford OX1 3RH, England
AND
DUNCAN A. FORBES[1]
Institute of Astronomy, Madingley Road, Cambridge CB3 0HA, England
Received 1992 June 16; accepted 1992 September 17

ABSTRACT

Images of the merging luminous IR galaxy NGC 6240 in the H_2 $v = 1 \rightarrow 0$ $S(1)$ 2.12 μm line and the [Fe II] 1.64 μm line are presented, together with velocity-resolved slit spectra of these lines. The images have an angular resolution of $\lesssim 1''$, and for the H_2 line, images in three adjacent 320 km s^{-1} wide velocity intervals are presented. The H_2 emission does not follow the stellar light and shows no trace of the two nuclei of the galaxy. Instead, it peaks *between* these nuclei. The H_2 emission extends over $\sim$5 kpc and shows a complex morphology and velocity structure in its outer parts. It is concluded that the bright H_2 emission near the nuclei is generated in shocks resulting from the collision of the interstellar media of the merging galaxies. Line ratios indicate that the shock velocity is at most 40 km s^{-1}. It is argued that a fast shock propagating in a low-density medium generates slower shocks in dense clouds, giving rise to the observed H_2 emission. It is shown that the shocks in NGC 6240 cannot account for the observed far-IR emission. High-velocity wings on the H_2 line profile (FWZI $\sim$ 1600 km s^{-1}) are interpreted as evidence for molecular material entrained in and shocked by the "superwind" in NGC 6240, created by multiple supernova explosions in a nuclear starburst. In contrast to the H_2 emission, the [Fe II] emission comes from the nuclei of the galaxy and is generated in fast supernova remnant (SNR) shocks in the nuclear starbursts. The high [Fe II]/Brγ ratio indicates a high gas-phase iron abundance, resulting from grain destruction in the SNR shocks. The high [Fe II]/Brγ, radio/Brγ and far-IR/Brγ ratios in NGC 6240 indicate a deficiency in stars more massive than $\sim$25 $M_\odot$, which can be accounted for by a decrease with time in nuclear star formation activity. This decrease may be due to the expulsion of molecular gas from the nuclei by the "superwind" created by the nuclear starburst, which is confirmed by the detection of high-velocity H_2 emission from material entrained in the superwind.

Subject headings: galaxies: individual (NGC 6240) — galaxies: interactions — galaxies: nuclei — galaxies: starburst — infrared: galaxies

1. INTRODUCTION

The peculiar galaxy NGC 6240 (UGC 10592, IC 4625, PKS 1650+024, IRAS 16504+0228) has been the subject of considerable study since the discovery of bright far-infrared emission from this system (Soifer et al. 1984a; Wright, Joseph, & Meikle 1984) during the *IRAS* mission. With its bolometric luminosity $L_{bol} \approx 6 \times 10^{11}\ L_\odot$ (for $H_0 = 75$ km s^{-1} Mpc^{-1}, as assumed throughout this paper, and $z = 0.0246$ for NGC 6240), dominated by far-infrared radiation, NGC 6240 belongs to the class of luminous infrared galaxies that were first discovered by *IRAS* (Soifer et al. 1984b). The origin of the high IR luminosities (up to $\sim 3.5 \times 10^{12}\ L_\odot$) of these objects has been the subject of considerable debate during the last decade. NGC 6240 has often been called a "prototypical" luminous IR galaxy (e.g., Wright, Joseph, & Meikle 1984; Joseph & Wright 1985; Fried & Ulrich 1985; Rieke et al. 1985; Heckman, Armus, & Miley 1987, 1990; Armus, Heckman, & Miley 1987, 1989, 1990) but has also been referred to as "remarkable," "exceptional," or even "a mystery" (Moorwood & Oliva 1988; Elston & Maloney 1990; Draine & Woods 1990). Obviously, there is no consensus on the nature of the physical processes behind the observed properties of NGC 6240, be they "prototypical" or "exceptional."

In this paper we attempt to clarify the situation concerning NGC 6240 by an analysis of new seeing-limited narrow-band images and velocity-resolved spectra of the H_2 and [Fe II] near-IR emission of this galaxy. In § 2 the observations are described, while the results are presented in § 3. In § 4 the results are analyzed and the origin of the H_2 and [Fe II] emission is discussed. Section 5 summarizes the conclusions. However, we begin by summarizing the current understanding of NGC 6240. Section 1.1 briefly discusses the various models that have been proposed to account for the far-IR luminosity of NGC 6240 and other luminous IR galaxies. The properties of NGC 6240 that make this galaxy stand out as a unique object, and the models that have been put forward to explain these features, are outlined in § 1.2.

1.1. *The Far-IR Luminosity of NGC 6240 and Its Origin*

It is usually assumed that the far-IR luminosity of luminous IR galaxies is powered by extraordinarily high numbers of massive stars, of which the UV radiation, after absorption by dust, is reradiated in the far-IR (e.g., Rieke & Low 1972; Telesco & Harper 1980). Since massive stars are short-lived,

[1] Present address: Lick Observatory, University of California, Santa Cruz, CA 95064.

the corresponding star formation rates are so high that the available gas in luminous IR galaxies would be exhausted in much less than a Hubble time if star formation were maintained at the high level required to power the far-IR emission (e.g., Scoville & Young 1983; Sanders & Mirabel 1985; Thronson & Telesco 1986). The relatively short periods of enhanced star formation thus inferred have been called "starbursts." It has been noted by many authors that a large percentage ($\gtrsim 70\%$) of all luminous IR galaxies are interacting or merging (Soifer et al. 1984b; Allen, Roche, & Norris 1985; Sanders & Mirabel 1985; Joseph & Wright 1985; Soifer et al. 1986; Sanders et al. 1988). This fact has been used to argue in favor of the starburst model for luminous IR galaxies, by interpreting the starburst as a direct result of the interaction. Indeed, Larson & Tinsley (1978) have presented evidence that galaxy interactions trigger massive star formation, since interacting galaxies were observed to be bluer than isolated galaxies. Theoretical support for this suggestion comes from combined numerical simulations of stellar dynamics and gas dynamics in interacting galaxies (Negroponte & White 1983; Noguchi 1988; Hernquist 1989; Olson & Kwan 1990). These simulations show that, owing to dynamic torques exerted by tidal forces during the galaxy interaction, the gaseous component, being more dissipative than the stellar component, quickly sheds most of its angular momentum and falls to the center of the potential well. The starburst scenario is further supported by the observational result that luminous IR galaxies contain large masses of molecular gas (up to $\sim 10^{11}\ M_\odot$) as shown by their high luminosities in the ^{12}CO $J = 1 \rightarrow 0$ line (see Young & Scoville 1991, their Fig. 7), most of which is concentrated in a $\lesssim 1$ kpc region near the nucleus, where it may even constitute the dominant mass component (Wang, Scoville, & Sanders 1991; Scoville et al. 1991; Okumura et al. 1991; Scoville & Soifer 1991). Furthermore, as shown by observations of HCN $J = 1 \rightarrow 0$ in a number of luminous IR galaxies, the fraction of molecular gas located in dense ($n_{H_2} \gtrsim 10^4$ cm^{-3}) molecular clouds is much higher in luminous IR galaxies than in less luminous systems such as our own Galaxy (Solomon, Downes, & Radford 1992). Finally, the tight correlation between nonthermal radio power and far-IR luminosity that holds for galaxies ranging from low-luminosity spirals and even star-forming E/S0 galaxies to the most luminous IR galaxies (Condon et al. 1982; Helou, Soifer, & Rowan-Robinson 1985; De Jong et al. 1985; Condon & Broderick 1986, 1988; Dressel 1988; Wrobel & Heeschen 1988) can be explained by the starburst model: the far-IR emission originates in dust heated by UV radiation from a large number of OB stars, while the same population of stars is responsible for the supernova shocks that produce the relativistic electrons giving rise to the observed synchrotron radio emission (e.g., Harwit & Pacini 1975; Condon & Yin 1990).

NGC 6240 is a luminous IR galaxy as well as a bright radio source. In spite of its in some respects remarkable properties (see § 1.2), its radio and far-IR emission are in agreement with the radio–far-IR correlation referred to above and can thus both be explained by the starburst model. A further argument that is often used in support of this interpretation is the fact that NGC 6240 is a merging system, since merging or interaction can trigger star formation (see above). Zwicky et al. (1961) were the first to draw attention to the disturbed visual appearance of NGC 6240, characterized by pronounced dust lanes and extended tails. Their widely accepted suggestion that this morphology is the result of a collision (e.g., Vorontsov-Vel'yaminov 1977; Fosbury & Wall 1979; Zasov & Karachentsev 1979) was confirmed more than 20 years later by Fried & Schulz (1983), who in their *I*- and *r*-band images of NGC 6240 detected two nuclei separated by 1".8. At the kinematic distance of 100 Mpc for NGC 6240 this separation corresponds to a projected distance of 0.9 kpc between the nuclei.

Although the merger nature of NGC 6240 and the fact that it follows the far-IR–ratio correlation are consistent with the starburst model, these arguments do not prove the correctness of this interpretation. It is therefore important to find direct indications for intense star formation in NGC 6240. The most convincing evidence has been provided by Lester, Harvey, & Carr (1988, hereafter LHC). These authors have detected strong CO overtone vibrational absorption at ~ 2.3 μm in the nuclear region of NGC 6240, and conclude that the light from the nucleus in this spectral region is dominated by a population of red supergiants created in a vigorous nuclear starburst. Further evidence for a starburst in these nuclei has been presented by Smith, Aitken, & Roche (1989), who observed the 7.7, 8.6, and 11.25 μm emission features in the NGC 6240 nuclei. These features are typically found in star-forming galaxies, where they are attributed to vibrational fluorescence of UV-pumped polycyclic aromatic hydrocarbons (PAHs) (Léger & Puget 1984; Allamandola, Tielens, & Barker 1985), but are not observed in active galactic nuclei (AGNs) (Aitken, Roche, & Phillips 1981; Moorwood 1986; Roche et al. 1991). Finally, an extended ($\sim 50 \times 60$ kpc) and morphologically complex halo around NGC 6240 has been observed by Heckman et al. (1987) and Armus et al. (1990) in narrow-band Hα + [N II] images. This halo is morphologically and spectrally similar to the Hα halo of the nearby starburst galaxy M82 (McCarthy, Heckman, & van Breugel 1987), which is interpreted as the result of a "superwind" driven by the multiple supernovae resulting from the starburst in the inner parts of the galaxy (Chevalier & Clegg 1985).

However, the starburst model for NGC 6240 is not without problems. Several authors have argued that the hydrogen recombination line intensities (even in the near-IR) in NGC 6240 are much lower than expected from a starburst containing a large number of massive stars powering the observed far-IR emission (DePoy, Becklin, & Wynn-Williams 1986; LHC; Keel 1990; Thronson et al. 1990), a phenomenon that has also been observed in some other luminous IR galaxies (Beck, Turner, & Ho 1986). This result has prompted several different (nonstarburst) interpretations for the observational properties of NGC 6240.

Harwit et al. (1987) have proposed that the strong emission of luminous IR galaxies is powered by the collisional heating of gas in strong galaxy interactions. In this model fast collisions ($v_s \sim 500$ km s^{-1}) between molecular clouds in the colliding galaxies will produce copious UV radiation, which after absorption by dust grains will be reradiated in the far-IR. Harwit et al. (1987) argue that a large fraction of the interaction energy can be converted into IR emission by this process, thus explaining the IR luminosity of these sources as well as the fact that most of them are interacting or merging systems. In this model the bright CO $J = 1 \rightarrow 0$ emission is due to the cooling of radiatively heated preshock molecular gas. The observed nonthermal radio emission is due to relativistic electrons accelerated at shock fronts generated in the colliding system. Since shocks produce generally lower ionization and excitation states than photoionization, this scenario provides a simple explanation for the weak hydrogen recombination line

intensities observed in NGC 6240. Furthermore, this model can account for the fact that the optical fine-structure spectrum of NGC 6240 is dominated by low-excitation and -ionization lines, and is typical of radiative shocks with velocities of a few hundred kilometers per second (Fosbury & Wall 1979; Kirhakos & Phillips 1989; Keel 1990). As such, the optical spectrum of NGC 6240 is probably the best-known example of a shock-excited low-ionization nuclear emission region (LINER) spectrum.

Finally, it has been proposed that the observed luminosity of some luminous IR galaxies is powered by a dust-enshrouded AGN, which would also produce the observed synchrotron radiation at radio wavelengths (e.g., Carral, Turner, & Ho 1990; Condon et al. 1991). This interpretation has been applied to NGC 6240 by DePoy et al. (1986) and by Thronson et al. (1990).

1.2. *Near-IR Spectral Lines in NGC 6240*

Spectral line observations in the H (1.65 μm) and K (2.2 μm) near-IR windows have revealed extraordinarily luminous emission from NGC 6240 in the H_2 $v = 1 \rightarrow 0$ $S(1)$ line at 2.121 μm and the [Fe II] $a^4D_{7/2} \rightarrow a^4F_{9/2}$ line at 1.644 μm. The exceptional properties of NGC 6240 in these lines can be summarized as follows:

1. The luminosity of NGC 6240 in the H_2 line is $\sim 8 \times 10^7$ $L_\odot$; in the [Fe II] line this value is $\sim 5 \times 10^7$ $L_\odot$, with no correction for extinction. These values are the largest currently known luminosities of any galaxy in these lines.
2. NGC 6240 has by far the largest known ratio of H_2 and [Fe II] flux to Brγ flux. While for most galaxies where the lines have been observed these ratios are of the order of unity (Moorwood & Oliva 1988), for NGC 6240 the ratios are H_2/Br$\gamma \sim 45$ and [Fe II]/Br$\gamma \sim 12$.
3. NGC 6240 has the largest known ratio of H_2 luminosity to bolometric luminosity. Since the H_2 $v = 1 \rightarrow 0$ $S(1)$ line probably contains at most 10% of the total vibrational emission of H_2, the total H_2 near-IR line luminosity accounts for more than $\sim 0.1\%$ of the bolometric luminosity of NGC 6240. In contrast, the ratio of [Fe II] to bolometric luminosity in this galaxy is not exceptionally high.

While the [Fe II] emission in NGC 6240 is usually attributed to fast ($v_s \gtrsim 100$ km s^{-1}) shocks (LHC; Moorwood & Oliva 1988; Elston & Maloney 1990), there is no agreement on the origin of the strong H_2 lines. Several authors suggest that the H_2 emission of NGC 6240 originates in shocked molecular gas. This model provides a simple explanation for the high H_2/Brγ ratio and is consistent with the observed thermal vibrational spectrum of the H_2, as observed by LHC. Moorwood & Oliva (1990) suggested shocks from supernova explosions accompanying a nuclear starburst as the origin of the H_2 emission. Rieke et al. (1985) first proposed that molecular gas shocked during the merging process produces the observed H_2 emission. The latter conclusion was supported by multiaperture measurements (LHC), long-slit spectroscopy (Elston & Maloney 1990), and narrow-band spectral line images (Fischer, Smith, & Glaccum 1990; Herbst et al. 1990, hereafter H+5), that showed the H_2 emission to be extended. The image presented by H+5 (their Fig. 2) shows that the H_2 emission does not follow the stellar light and that the position of brightest H_2 emission is located *between* the two nuclei of the merging galaxies. This morphology is difficult to reconcile with shock excitation by supernova explosions (where the H_2 emission would be expected to follow the stellar light) and can be interpreted as evidence for large-scale shocks in the colliding molecular components of the merging galaxies.

Several alternative mechanisms have been proposed to account for the observed brightness of the H_2 lines. Tanaka, Hasegawa, & Gatley (1991) argue that UV electronic excitation followed by vibrational fluorescence can account for the observed H_2 spectrum and luminosity. The required UV radiation is supplied by the starburst, which must, however, be strongly deficient in O stars, in order to explain the high H_2/Brγ ratio.

Finally, Draine & Woods (1990) have suggested that the absorption of a significant soft X-ray flux by the molecular clouds in NGC 6240 will result in extended zones of warm gas that cool by rotational and vibrational emission of H_2. The observed H_2 luminosity and spectrum can be produced if $\sim 10^{10}$ $L_\odot$ of soft X-rays is being absorbed by the molecular component of NGC 6240. These X-rays can be produced by supernova explosions at a rate of ~ 7 yr^{-1} (Draine & Woods 1991), or by high-velocity shocks between molecular clouds, resulting from the merging process.

2. OBSERVATIONS AND REDUCTION

2.1. *Imaging Spectroscopy*

NGC 6240 was observed on 1991 July 20, 25, and 27 and August 3 with the Max-Planck-Institut für Extraterrestrische Physik (MPE) Fabry-Perot Array Spectrometer (FAST; Rotaciuc 1992; Krabbe et al. 1993) at the 4.2 m William Herschel Telescope (WHT) of the Royal Greenwich Observatory at the Observatorio del Roque de Los Muchachos on La Palma, Canary Islands. FAST is a near-IR camera optimized for K-band observations, equipped with a 58 × 62 pixel InSb detector array manufactured by Santa Barbara Research Corporation. The camera was used at the f/11 Cassegrain focus of the WHT, with an image scale of 0.″5 pixel^{-1} and no vignetting over the entire 0.′5 field of view. The helium-cooled array was operated at a temperature of 6 K, yielding a typical dark current of ~ 50 electrons s^{-1} and readout noise of $\lesssim 280$ electrons. Spectral dispersion was provided by a cold circular variable filter (CVF) covering the wavelength range from 1.4 to 2.4 μm, and a warm Queensgate Instruments, Ltd., tunable Fabry-Perot etalon at the telescope focal plane, operating in the 2.0–2.4 μm wavelength range. Observations with the Fabry-Perot ($\lambda/\Delta\lambda = 950$, corresponding to a velocity resolution of 320 km s^{-1}) were carried out with the CVF ($\lambda/\Delta\lambda = 45$) used as order sorter. Wavelength calibration was achieved by scanning the CVF and Fabry-Perot over bright near-IR lines in the arc spectrum of an argon lamp.

Three near-IR spectral lines were observed in NGC 6240: the H_2 $v = 1 \rightarrow 0$ $S(1)$ line (rest wavelength $\lambda_0 = 2.121$ μm), the He I $2^1P \rightarrow 2^1S$ line ($\lambda_0 = 2.058$ μm), and the [Fe II] $a^4D_{7/2} \rightarrow a^4F_{9/2}$ line ($\lambda_0 = 1.644$ μm). These measurements were carried out by taking narrow-band images in these lines at the systemic velocity of the galaxy, plus narrow-band images of the adjacent continuum on either side of the line. For the H_2 line, images at velocities displaced by +280 km s^{-1} and −280 km s^{-1} from the systemic velocity of the galaxy (v_{sys}) were obtained as well. A value $v_{sys} = 7390$ km s^{-1} was used, as measured by Fried & Ulrich (1985) from optical emission lines from the brightest nucleus of NGC 6240. For the H_2 and He I lines, the Fabry-Perot was used with the CVF as predisperser, while for the [Fe II] line only the CVF was used. Typical

exposure times ranged from 100 to 300 s. Total on-line integration times were 2000 s on the H_2 line at the center velocity (plus 800 s on each of the two velocity-shifted channels), 900 s on the He I line, and 2000 s on the [Fe II] line. Seeing conditions were excellent, with subarcsecond ($\approx$0".7–1".0) K-band seeing during the [Fe II] and He I observations, and during a substantial part of the H_2 observations. The observations were complemented by measurements of the standard stars HD 161903 (spectral type A2, $m_K = 7.02$ mag, $m_H = 7.055$ mag), HD 162208 (spectral type A0, $m_K = 7.11$ mag, $m_H = 7.145$ mag) and HR 6136 (spectral type K4 III, $m_K = 2.03$ mag, $m_H = 2.16$ mag), which were observed at the same air mass as NGC 6240. Flat-field frames were obtained from long exposures on blank sky through the CVF.

The data reduction was carried out using the MIDAS package (release JAN88). Standard procedures were used for the removal of hot and cold pixels and cosmic ray hits, dark-current subtraction, and flat-fielding. Atmospheric features were removed by dividing by the observed standard star spectra. Individual exposures were aligned by requiring their peak positions to coincide. Finally, continuum images constructed from the off-line images taken on either side of the line were removed from the on-line frames, yielding pure line images. This subtraction also effectively removed any atmospheric foreground emission.

2.2. *Long-Slit Spectroscopy*

The imaging spectroscopy was supplemented with long-slit spectroscopy, using the near-infrared grating spectrometer IRSPEC (Moorwood, Moneti, & Gredel 1991; see also Koornneef 1993) on the New Technology Telescope (NTT) of the European Southern Observatory (ESO), La Silla, Chile, in 1992 June. The slit was centered on the nuclei of NGC 6240 and oriented north-south, with a slit width of 4".4. The pixel scale on the spatial axis was 2".2. Four lines were observed in NGC 6240: the H_2 $v = 1 \rightarrow 0$ $S(1)$ line (rest wavelength $\lambda_0 = 2.121$ μm), the H_2 $v = 1 \rightarrow 0$ $S(3)$ line ($\lambda_0 = 1.957$ μm), the [Fe II] $a^4D_{7/2} \rightarrow a^4F_{9/2}$ line ($\lambda_0 = 1.644$ μm), and the [Fe II] $a^4D_{7/2} \rightarrow a^6D_{9/2}$ line ($\lambda_0 = 1.257$ μm). Individual 120 s exposures alternated between source and sky positions. Total integration times ranged from 240 s for the H_2 $v = 1 \rightarrow 0$ $S(1)$ line to 3840 s for the [Fe II] line at 1.257 μm. The spectral resolution as measured from unresolved OH airglow lines was consistent with the theoretical spectral resolution of IRSPEC: $\lambda/\Delta\lambda = 1880$ for the H_2 $v = 1 \rightarrow 0$ $S(1)$ line, 1650 for the $S(3)$ line, 1350 for the [Fe II] 1.644 μm line, and 1520 for the [Fe II] 1.257 μm line. The corresponding FWHM velocity resolutions of 160, 180, 220, and 200 km s^{-1}, respectively, are sufficient to resolve the lines easily. Wavelength calibration was achieved with an internal neon lamp. Comparison with observed airglow lines of vibrationally excited OH (Oliva & Origlia 1992) showed this calibration to be better than 1 pixel in the dispersion direction. The observations were complemented with short exposures on the stars HR 6195 (spectral type A1 V, $m_J = 5.73$ mag, $m_H = m_K = 5.71$ mag) and HR 6378 (η Oph, spectral type A2 V, $m_J = 2.33$ mag, $m_H = m_K = 2.30$ mag), at the same air mass at NGC 6240.

The spectra were reduced with the MIDAS package (release NOV91). Standard procedures were used for the removal of hot and cold pixels, dark-current subtraction, flat-fielding, and subtraction of atmospheric foreground emission. Atmospheric absorption features were removed by dividing by the observed standard star spectra, which were first corrected for the presence of photospheric hydrogen Brackett and Paschen lines. Finally, the data were integrated along the spatial axis to yield spectra integrated over a north-south strip centered on the nuclei of NGC 6240 and 4".4 wide in right ascension.

3. RESULTS

3.1. H_2 *Results*

3.1.1. H_2 *Morphology*

The three H_2 channel maps obtained with FAST are shown in Figures 1*a*–1*c*. It is immediately clear that, unlike the stellar light (and several other tracers; see below), the H_2 emission does *not* show the two nuclei of NGC 6240. Instead, one broad peak is seen that has a FWHM of 1".7 (800 pc) in right ascension and of 2".3 (1100 pc) in declination and is thus clearly resolved. The location of this peak with respect to the nuclei of the galaxy was determined by inspecting the continuum images on either side of the line. It is concluded that the peak of the H_2 emission is located *between* the two nuclei of NGC 6240. This remarkable result is shown in Figure 2 (Plate 4). This figure shows the [Fe II] 1.64 μm emission, which originates in the nuclei of NGC 6240 (see § 3.2), overlaid on an image of the velocity-integrated H_2 $v = 1 \rightarrow 0$ $S(1)$ emission. As will be discussed in § 4.1, the geometry shown in Figure 2 is of crucial importance for understanding the origin of the H_2 emission from the central region of NGC 6240.

The morphology of our central channel is in agreement with that found by H+5, who also conclude that the H_2 peak is located between the two nuclei. However, the image shown in Figure 1*b* is approximately a factor of 3 deeper, as can be seen from the lowest contour in the image by H+5, which corresponds to the third (1×10^{-4} ergs s^{-1} cm^{-2} sr^{-1}) contour in Figure 1*b*. At these brightness levels a complex structure of tails and extensions is visible. While the image by H+5 shows only the brightest two of these tails (those southwest and southeast of the peak position), Figure 1*b* suggested the presence of several additional, fainter extensions, in particular in the northern and eastern regions. Some of these features are also seen in the lower resolution H_2 image published by Fischer et al. (1990). The fainter H_2 features extend to $\approx$5" (2.5 kpc) from the peak. The total projected extent of the H_2 emission is thus $\approx$5 kpc, in agreement with estimates from multi-aperture measurements by LHC, from long-slit spectroscopy by Elston & Maloney (1990), and from the narrow-band image by Fischer et al. (1990). In its outer parts the H_2 emitting region shows a general resemblance to the Hα images published by Heckman et al. (1987), Armus et al. (1990), and Keel (1990), in particular in the area of the southeast and southwest tails. However, in the central region the Hα shows the two nuclei of NGC 6240 (as shown most clearly by Keel 1990), whereas the H_2 emission peaks between those nuclei, as shown in Figure 2. Thus only in the outer regions of the area detected in H_2 is a morphological similarity of H_2 and Hα emission found.

The total H_2 line flux in the present data, integrated over the emitting area and summed over all three velocity channels is 2.7×10^{-13} ergs s^{-1} cm^{-2}. Table 1 compares this value with previous measurements. Our flux measurement is near the average of the previous determinations and is in excellent agreement with the results from the long-slit spectroscopy by Elston & Maloney (1990). The integrated flux obtained by H+5 is lower than most of the other results, which may result from the lack of faint extended emission in their image.

PLATE 4

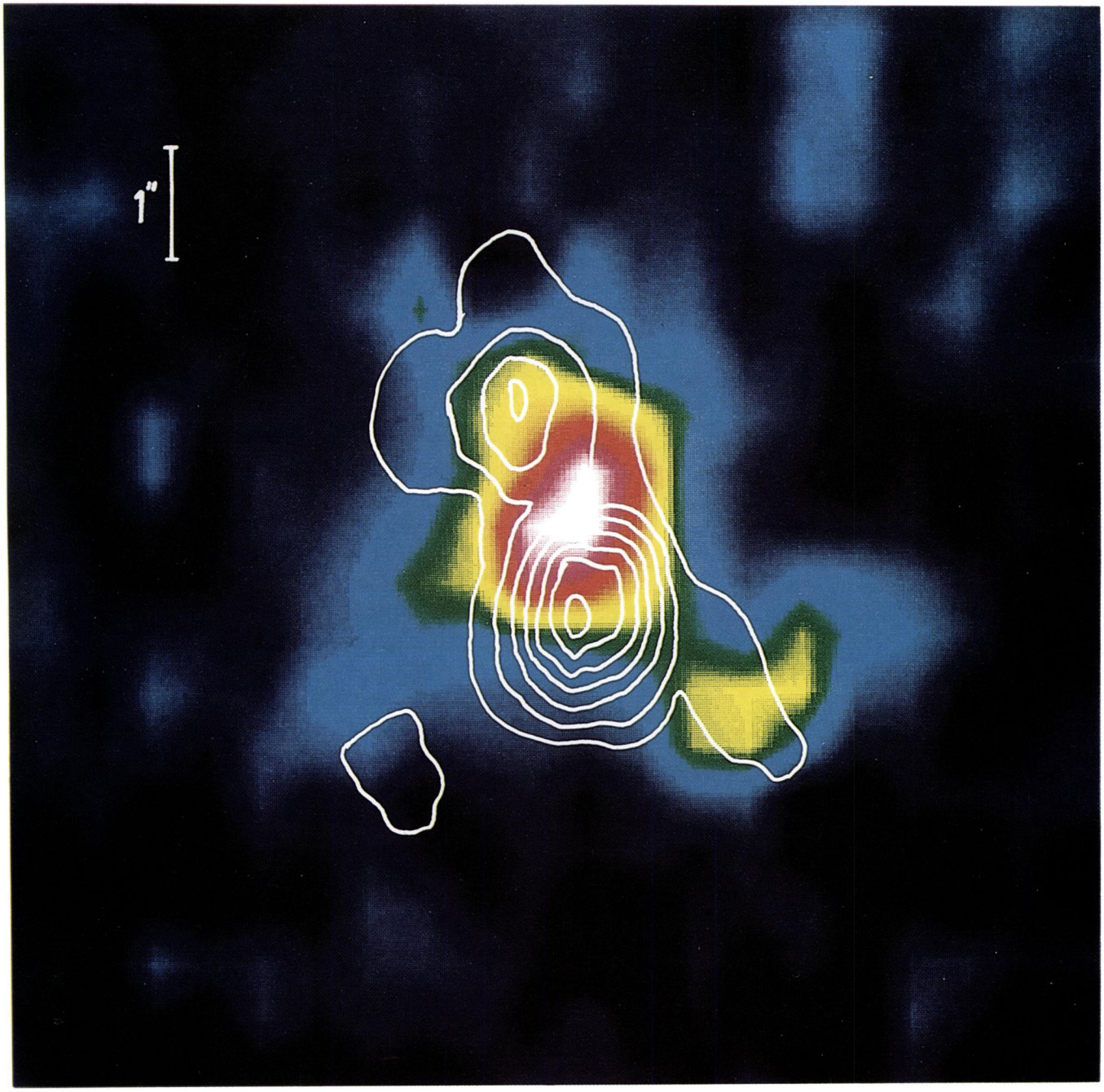

FIG. 2.—False color representation of the velocity-integrated H_2 $v = 1 \rightarrow 0$ $S(1)$ line emission from NGC 6240, with a contour representation of the [Fe II] 1.64 μm emission overlaid. Contour levels are as in Fig. 4.

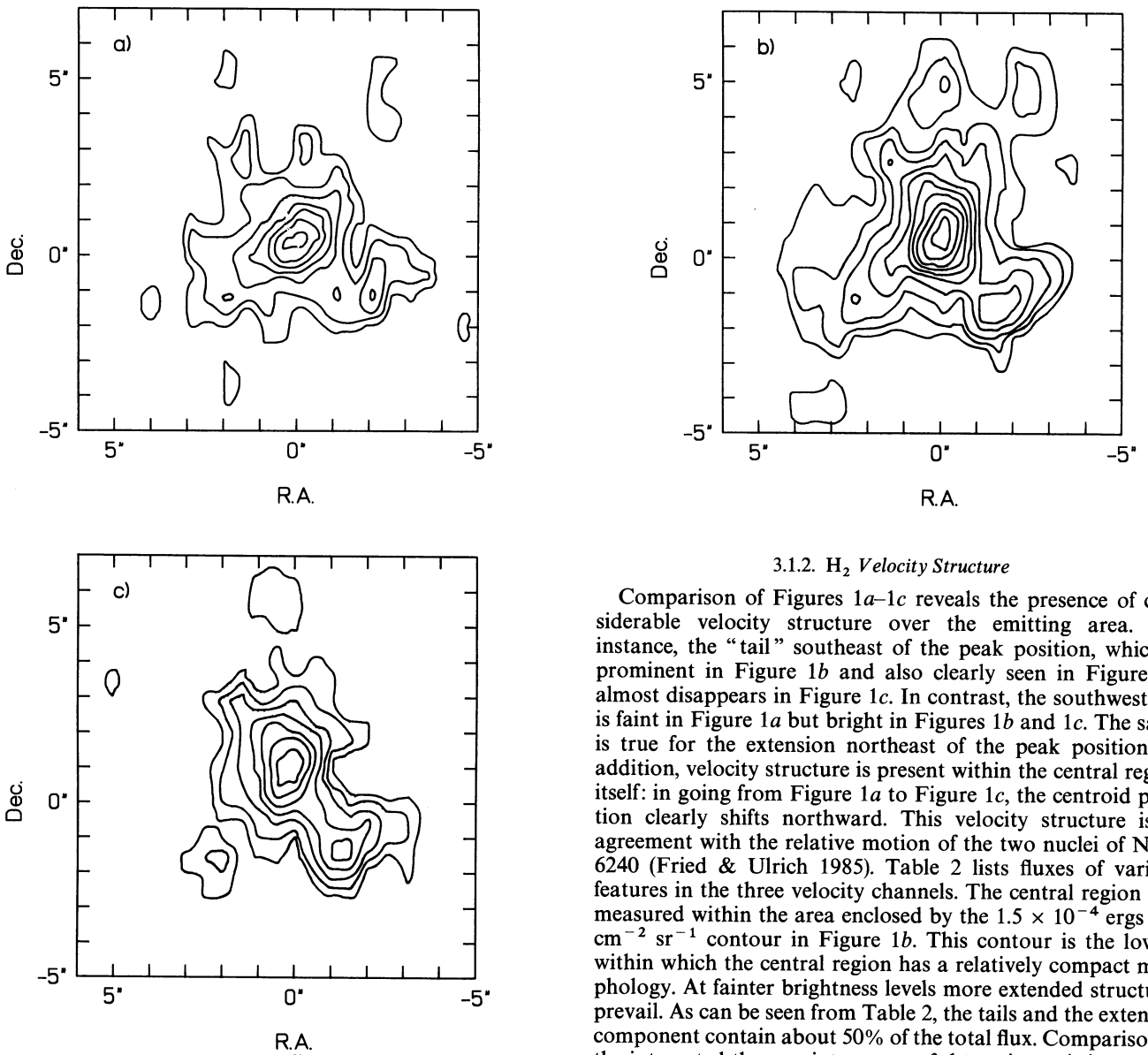

FIG. 1.—H_2 $v = 1 \rightarrow 0$ $S(1)$ line emission from NGC 6240 at three velocities: (*a*) $v_{sys} - 280$, (*b*) v_{sys}, and (*c*) $v_{sys} + 280$, where $v_{sys} = 7390$ km s^{-1} is the systemic velocity of NGC 6240. Contour levels are 0.3, 0.6, 1.0, 1.5, 2.0, 2.5, 3.0, 3.6, 4.2, and 5.0 $\times$ 10^{-4} ergs s^{-1} cm^{-2} sr^{-1}.

3.1.2. H_2 *Velocity Structure*

Comparison of Figures 1*a*–1*c* reveals the presence of considerable velocity structure over the emitting area. For instance, the "tail" southeast of the peak position, which is prominent in Figure 1*b* and also clearly seen in Figure 1*a*, almost disappears in Figure 1*c*. In contrast, the southwest tail is faint in Figure 1*a* but bright in Figures 1*b* and 1*c*. The same is true for the extension northeast of the peak position. In addition, velocity structure is present within the central region itself: in going from Figure 1*a* to Figure 1*c*, the centroid position clearly shifts northward. This velocity structure is in agreement with the relative motion of the two nuclei of NGC 6240 (Fried & Ulrich 1985). Table 2 lists fluxes of various features in the three velocity channels. The central region was measured within the area enclosed by the 1.5 $\times$ 10^{-4} ergs s^{-1} cm^{-2} sr^{-1} contour in Figure 1*b*. This contour is the lowest within which the central region has a relatively compact morphology. At fainter brightness levels more extended structures prevail. As can be seen from Table 2, the tails and the extended component contain about 50% of the total flux. Comparison of the integrated three-point spectra of the entire emitting region and of the southwest tail with the corresponding spectra presented by H + 5 shows good agreement. However, the conclusion by H + 5 that no significant velocity structure exists over the emitting area is in disagreement with the present data. We suggest that the discrepancy with H + 5 arises because much of

TABLE 1

PRESENT AND PREVIOUS MEASUREMENTS OF THE TOTAL H_2 $v = 1 \rightarrow 0$ $S(1)$ FLUX FROM NGC 6240

H_2 $v = 1 \rightarrow 0$ $S(1)$ Flux (ergs s^{-1} cm^{-2})	Method	Reference
1.5 $\times$ 10^{-13}	5".5 aperture spectroscopy	Joseph, Wright, & Wade 1984
3.9 $\times$ 10^{-13}	8".7 aperture spectroscopy	Rieke et al. 1985
1.8 $\times$ 10^{-13}	5".5 aperture spectroscopy	DePoy, Becklin, & Wynn-Williams 1986
2.1 $\times$ 10^{-13}	6".0 aperture spectroscopy	Moorwood & Oliva 1988
1.3 $\times$ 10^{-13}	3".0 aperture spectroscopy	Lester, Harvey, & Carr 1988
2.8 $\times$ 10^{-13}	Long-slit spectroscopy	Elston & Maloney 1990
1.9 $\times$ 10^{-13}	Imaging	Fischer, Smith, & Glaccum 1990
1.3 $\times$ 10^{-13}	Imaging	Herbst et al. 1990
2.7 $\times$ 10^{-13}	Imaging	This work

TABLE 2

H_2 $v = 1 \rightarrow 0$ $S(1)$ FLUXES OF FEATURES IN NGC 6240 IN INDIVIDUAL 320 km s^{-1} WIDE CHANNELS

FEATURE	H_2 $v = 1 \rightarrow 0$ $S(1)$ FLUX (ergs s^{-1} cm^{-2})		
	$v_{sys} - 280$	v_{sys}	$v_{sys} + 280$
Central region[a]	2.5×10^{-14}	6.4×10^{-14}	3.6×10^{-14}
Southwest tail	0.2×10^{-14}	1.2×10^{-14}	0.9×10^{-14}
Southeast tail	0.5×10^{-14}	2.0×10^{-14}	0.1×10^{-14}
Northeast tail	0.3×10^{-14}	1.9×10^{-14}	2.2×10^{-14}
Total[b]	0.5×10^{-13}	1.3×10^{-13}	0.9×10^{-13}
Extended[c]	1.2×10^{-14}	2.4×10^{-14}	2.2×10^{-14}

[a] Integrated within 1.5×10^{-4} ergs s^{-1} cm^{-2} sr^{-1} contour in Fig. 1*b*. The same area was used in all three channels.
[b] Integrated over entire emitting area.
[c] Calculated: total − (central region + tails).

the velocity structure occurs at lower brightness levels, which may have been missed by H + 5, as indicated by the low total flux found by these authors.

The H_2 spectra obtained with IRSPEC are shown in Figure 3. The lines are clearly resolved. For the H_2 $v = 1 \rightarrow 0$ $S(1)$ line (Fig. 3*a*) a FWHM of 550 km s^{-1} is obtained (after correction for the instrumental profile), in excellent agreement with the widths measured by DePoy et al. (1986), LHC, and Elston & Maloney (1990), and much higher than the FWHM of 320 km s^{-1} measured in the ^{12}CO $J = 1 \rightarrow 0$ line (Wang et al. 1991). The line profile is distinctly non-Gaussian: it is asymmetric and possesses wings on either side of the peak, but most prominently at the long-wavelength side. The zero-intensity points are displaced from the peak position by 620 km s^{-1} at the short-wavelength side and by 980 km s^{-1} at the long-wavelength side, yielding a total full width at zero intensity (FWZI) of 1600 km s^{-1}. The H_2 $v = 1 \rightarrow 0$ $S(3)$ line (Fig. 3*b*) has a profile that, within the uncertainties caused by atmospheric features in this wavelength region, is identical to that of the $S(1)$ line, showing the same line wings and asymmetry. While the large FWHM of the line cores had been observed before (see above) and the asymmetry had been noticed by H + 5, the detection of the high-velocity wings is a new result. This detection suggests a relation between the high-velocity material producing the H_2 line wings and the extended ionized halo associated with NGC 6240, which has a typical FWHM of ~1000 km s^{-1} in Hα in the central few kiloparsecs (Heckman et al. 1990). This interpretation is corroborated by the fact that most of the velocity structure in H_2 is seen in the extended tails also observed in Hα (cf. § 3.1.1). Table 2 shows that the southeast tail is blueshifted with respect to the central region, while the southwest tail and northeast tails are redshifted, the latter by ~200 km s^{-1}. We note that this velocity structure cannot be understood by simple rotation.

3.2. [Fe II] *Results*

The [Fe II] image is shown in Figure 4. The most striking feature of this image is its resemblance to the nuclear continuum emission, in sharp contrast to the H_2 images presented in § 3.1.1. Comparison with the off-line continuum images confirms that the two features seen in the [Fe II] image coincide in position with the two stellar nuclei of NGC 6240. The total [Fe II] line fluxes are 5.3×10^{-14} ergs s^{-1} cm^{-2} for the (optically brightest) southern nucleus and 3.3×10^{-14} ergs s^{-1} cm^{-2} for the northern one. Integrating our image in a 6″ aperture yields a total flux of 1.0×10^{-13} ergs s^{-1} cm^{-2}, indicating the presence of 1.4×10^{-14} ergs s^{-1} cm^{-2} in an extended component. Table 3 compares these values with previous measurements. Our total [Fe II] flux is low compared with most previous measurements, but agrees well with the measurement by LHC. Again the increase in flux with increasing aperture size suggests the presence of extended emission. Comparing our flux with the measurement of Moorwood & Oliva (1988), an extended component containing $\sim 7 \times 10^{14}$ ergs s^{-1} cm^{-2} in a 6″ aperture may be present, corresponding to an average brightness of $\sim 8 \times 10^{-5}$ ergs s^{-1} cm^{-2} sr^{-1}. This brightness level is less than the rms fluctuations in the background of our image, and could thus easily be lost in the background.

A velocity-resolved IRSPEC spectrum of the [Fe II] 1.644 μm line is shown in Figure 5. Although a very slight asymmetry toward the long-wavelength side may be present in the line profile, the [Fe II] line is much more nearly Gaussian than the H_2 lines shown in Figure 3. The FWHM (after correction for the instrumental profile) is 630 km s^{-1}, in excellent agreement with the value measured by Elston & Maloney (1990). This value is similar to the FWHM measured for the cores of the H_2 lines. However, the high-velocity wings of the H_2 lines are not

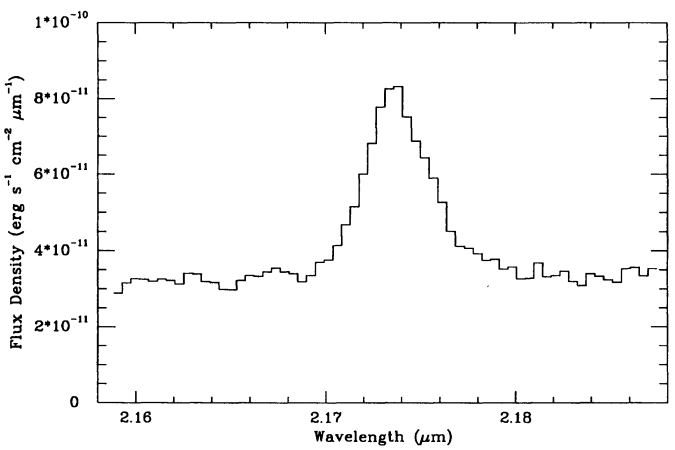

FIG. 3*a*

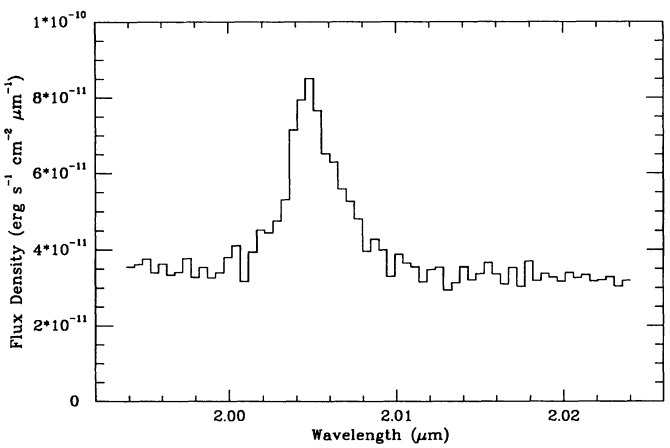

FIG. 3*b*

FIG. 3.—Velocity resolved spectra of H_2 vibrational line emission from NGC 6240. (*a*) H_2 $v = 1 \rightarrow 0$ $S(1)$ line. (*b*) H_2 $v = 1 \rightarrow 0$ $S(3$ line).

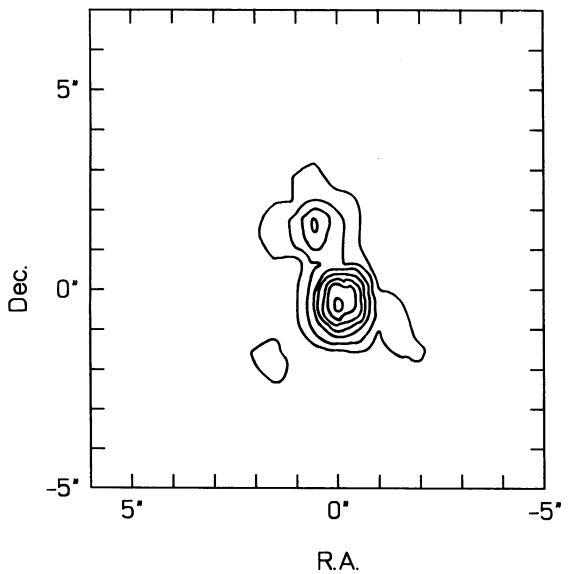

FIG. 4.—[Fe II] $a^4D_{7/2} \rightarrow a^4F_{9/2}$ line emission from NGC 6240. Contours are drawn at 2, 4, 6, 8, 10, 12, and 15 × 10^{-4} ergs s^{-1} cm^{-2} sr^{-1}.

present in the [Fe II] lines. The profile of the [Fe II] 1.257 μm line (not shown) is consistent with that of the 1.644 μm line. Total fluxes are 7.1 × 10^{-14} ergs s^{-1} cm^{-2} for the 1.644 μm line (this value is somewhat lower than the total flux contained in the image shown in Fig. 4) and 7.4 × 10^{-14} ergs s^{-1} cm^{-2} for the 1.257 μm line.

3.3. *Nondetections*

The He I line at 2.058 μm was not detected in NGC 6240. Upper limits (2 σ) of 8 × 10^{-5} ergs s^{-1} cm^{-2} sr^{-1} in brightness, of 2.5 × 10^{-15} ergs s^{-1} cm^{-2} in flux, and of 8 × 10^5 $L_\odot$ in luminosity in this line from the two nuclei are obtained. Our nondetection is consistent with the absence of the optical line of He I at 5876 Å (Fosbury & Wall 1979). We also note the absence of the [Si VI] $^2P_{3/2} \rightarrow {}^2P_{1/2}$ 1.962 μm line, which (if present) should have appeared in Figure 3*b* at 2.010 μm. Bright emission in this line has been found in some AGNs (e.g., Oliva & Moorwood 1990).

4. DISCUSSION

A striking feature of the data presented in the preceding sections is the contrasting morphology of the H_2 and the [Fe II] emission from NGC 6240, as shown most clearly by Figure 2. This pronounced difference indicates that different mechanisms give rise to the observed H_2 and [Fe II] emission, and warrants the separate analysis of these two tracers. Thus the H_2 emission will be discussed in § 4.1, while § 4.2 analyzes

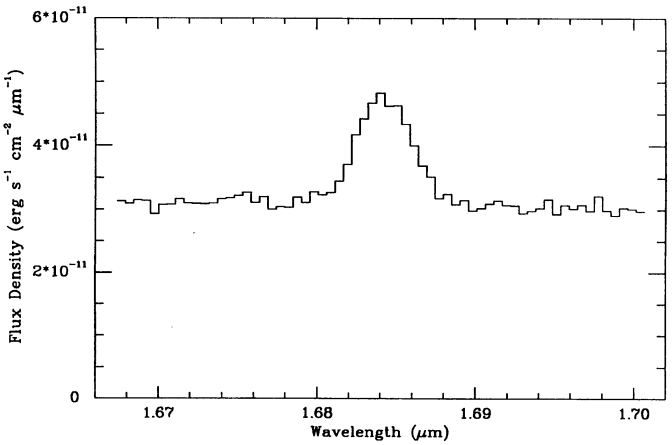

FIG. 5.—Velocity-resolved spectrum of the [Fe II] 1.644 μm line from NGC 6240.

the [Fe II] emission. The starburst properties of NGC 6240 will be discussed in § 4.3.

4.1. H_2 *Morphology and Kinematics: Collision Shock and Superwind*

The most remarkable feature of the H_2 image shown in Figure 2 is the fact that, *unlike any other tracer* observed at this resolution, it does *not* show any sign of the two nuclei of the galaxy. This conclusion has direct implications for the excitation mechanism of the H_2 emission. Most important, the observed H_2 morphology makes it extremely unlikely that stars are responsible for the H_2 excitation, since in that case the brightest H_2 emission would be expected from regions where the steller density is highest, i.e., from the nuclei of the galaxy. Such a morphology would be expected if UV excitation followed by near-IR fluorescence (as proposed by Tanaka et al. 1991), excitation by outflows from newly formed stars or by supernova remnant (SNR) shocks (as suggested by Moorwood & Oliva 1990), or excitation by X-rays produced in SNRs (Draine & Woods 1990) were responsible for the observed H_2 emission. The fact that the observed distribution of the H_2 emission is completely different from the stellar continuum emission is a strong argument against these excitation mechanisms.

In order to answer the question of what mechanisms *can* account for the observed H_2 morphology, we note that the H_2 emission is characterized by four features:

1. A broad peak, located *between* the remnant nuclei of the merging galaxies.
2. A number of extended features (" tails "), reaching projected distances of several kiloparsecs from the peak position.

TABLE 3

PRESENT AND PREVIOUS MEASUREMENTS OF THE TOTAL [Fe II] 1.64 μm FLUX FROM NGC 6240

[Fe II] 1.64 μm Flux (ergs s^{-1} cm^{-2})	Method	Reference
1.6 × 10^{-13}	6".0 aperture spectroscopy	Moorwood & Oliva 1988
1.0 × 10^{-13}	3".0 aperture spectroscopy	Lester, Harvey, & Carr 1988
2.1 × 10^{-13}	Long-slit spectroscopy	Elston & Maloney 1990
1.0 × 10^{-13}	Imaging	This work

3. A complex velocity structure in the outer parts that cannot be explained by a simple model such as ordered rotation.

4. The presence of emission at high velocities, giving rise to a FWZI of 1600 km s^{-1} for the H_2 line profile.

The location of the H_2 peak between the two nuclei unambiguously indicates that *the observed H_2 emission near the nuclei is excited by shocks generated in the collision of the nuclear interstellar media of the two merging galaxies.* This conclusion agrees with earlier work by LHC, Elston & Maloney (1990), and H+5. Large-scale shocks generated during the merging process can account naturally for most of the observed H_2 properties. In the first place, the fact that the position of brightest H_2 emission is located *between* the nuclei of the two merging galaxies is due to the fact that the densest regions of the two interstellar media are found close to the nuclei. Hence the most efficient dissipation of shock energy is taking place at the position where the nuclear interstellar media collide, i.e., *between* the nuclei. The complicated velocity structure of the emitting H_2, especially in the tails, may in this context be simply understood if the redshifted features are originally related to the galaxy with the receding (northern) nucleus, and the remaining features come originally from the other (approaching) galaxy with the southern nucleus. Finally, the large spatial extent ($\sim$5 kpc in projection) of the H_2 emission argues against any localized origin for the H_2 emission, but can be reproduced by large-scale shocks generated in the global collision of the two interstellar media.

The collision of the two interstellar media of the merging galaxies can thus account for the first three of the features of the H_2 emission that were listed above. However, the presence of high-velocity material at up to 900 km s^{-1} with respect to the systemic velocity of the galaxy at the long-wavelength side canot be explained in this context. In the first place, the interaction velocity of the two nuclei along the line of sight is only $\sim$150 km s^{-1} (Fried & Ulrich 1985). Second, if the interstellar media collided at a velocity much higher than $\sim$150 km s^{-1}, which would be required to produce the high-velocity H_2 line wings, energy dissipation at the shock front would be so rapid that the colliding media would be ionized and individual clouds would be destroyed (e.g., Harwit et al. 1987; Jog & Solomon 1992). It is therefore unlikely that the highest velocity H_2 emission is created in the shock generated by the collision of the two interstellar media. Instead, the general morphological agreement of the high-velocity H_2 "tails" with similar features seen in Hα (Heckman et al. 1987; Armus et al. 1990; Keel 1990) and the large width of the Hα profiles in the central few kiloparsecs (Heckman et al. 1990) indicate a common origin of the high-velocity H_2 and Hα emission. As argued by Heckman et al. (1990) on the basis of morphological, kinematic, and spectral evidence, this high-velocity gas is most likely propelled outward in a "superwind" driven by multiple supernovae resulting from a starburst in the nuclei of the galaxy. Molecular material entrained in and shocked by this superwind then accounts for the highest velocity H_2 emission. We thus conclude that the bright H_2 emission near the nuclei of NGC 6240 results from the collision of the two nuclear interstellar media of the merging galaxies, while the fainter H_2 emission in the "tails" of the H_2 emitting region may result from material accelerated and shocked by the superwind resulting from the nuclear starburst.

Collision shocks have been proposed as the origin of the H_2 emission from luminous IR galaxies by Harwit et al. (1987; see § 1.1 above). These authors argue that the far-IR emission is also generated in these shocks. Thus our conclusion that the brightest H_2 emission is powered by a global shock generated during the merging process raises an important question: is the far-IR emission of NGC 6240 also powered by the collision between the two interstellar media, as suggested by Harwit et al. (1987)? If the far-IR emission from NGC 6240 could indeed be powered by energy dissipation in shocks, there is no need to invoke the existence of a starburst in this galaxy. In that case the low recombination line flux (cf. § 1.1) would be quite natural. Such a conclusion would have important implications, since it would demonstrate the possibility of explaining the far-IR luminosity of luminous IR galaxies without invoking the presence of a starburst or an embedded AGN. In order to decide whether or not the shocks that produce the bright H_2 emission can also account for the far-IR luminosity, the nature of the shocks in NGC 6240 will be investigated in more detail in the next section.

4.1.1. *Shock Models and the Observed H_2 Line Emission*

As constraints for the various possible models the observed H_2 luminosity of NGC 6240 and the H_2/Brγ ratio will be used. The values of these two quantities will first be discussed.

The weakness of Brγ in NGC 6240 has made this line difficult to detect with certainty. Furthermore, because the H_2 lines are so strong, confusion of the faint Brγ line with the nearby H_2 $v = 2 \rightarrow 1$ $S(2)$ line is a problem. Published Brγ fluxes cover about an order of magnitude: 3.1×10^{-14} ergs s^{-1} cm^{-2} (Rieke et al. 1985; 8.″7 aperture), 6×10^{-15} ergs s^{-1} cm^{-2} (LHC; 3″ aperture), $< 6 \times 10^{-15}$ ergs s^{-1} cm^{-2} (3 σ upper limit; Moorwood & Oliva 1988; 6″ aperture), and 1.8×10^{-14} ergs s^{-1} cm^{-2} (Elston & Maloney 1990; long-slit spectroscopy). The Brγ flux may also be derived from other recombination lines. DePoy et al. (1986) have detected a Paα flux of 6.8×10^{-14} ergs s^{-1} cm^{-2} from NGC 6240. Assuming no reddening from Paα to Brγ and case B recombination (Lyman lines optically thick; Baker & Menzel 1938) the corresponding Brγ flux is 7×10^{-15} ergs s^{-1} (Hummer & Storey 1987), in agreement with the measurement by LHC. Therefore, adopting this value for the Brγ flux, a ratio H_2 $v = 1 \rightarrow 0$ $S(1)$/Br$\gamma \approx 45$ results. With a K-band extinction of 0.15 mag (Thronson et al. 1990), an intrinsic flux of 3.1×10^{-13} ergs s^{-1} cm^{-2} and an intrinsic luminosity of 9.7×10^7 $L_\odot$ for the H_2 $v = 1 \rightarrow 0$ $S(1)$ line are obtained.

We are now ready to consider the question whether or not a collision shock producing the observed H_2 emission and H_2/Brγ ratio can also produce the observed far-IR emission from NGC 6240. The conversion of part of the mechanical energy of a shock wave into vibrational H_2 line emission can proceed in various ways, each producing a particular H_2, Brγ, and far-IR flux for a given set of physical parameters. Four mechanisms are considered below.

1. Hollenbach & McKee (1989) have considered fast (v_s = 30–150 km s^{-1}) J-type shocks in molecular clouds with preshock densities n_0 ranging from 10^3 to 10^6 cm^{-3}. In their model the H_2 is initially completely dissociated, but subsequently re-forms in the cooling postshock gas. Formation of H_2 in excited vibrational states is the dominant mechanism of populating the vibrational levels. Far-IR emission is produced by grains heated collisionally in the hot postshock gas.

2. Draine, Roberge, & Dalgarno (1983) have modeled C-type shocks in molecular clouds (v_s = 5–50 km s^{-1}, n_0 =

10^2–10^6 cm^{-3}). In these shocks all hydrodynamic variables are continuous (Draine 1980), and peak temperatures are much lower than for J-shocks. Consequently, much less far-IR emission from dust grains is produced and H_2 is not dissociated. H_2 vibrational emission is produced in a layer where the fluid of ions and electrons moves through the neutral gas, thus heating the gas by ambipolar diffusion.

3. Harwit et al. (1987) have proposed that shocks generated in the collision of the interstellar media of two colliding or merging galaxies produce vibrational emission from collisionally excited H_2 in a layer of radiatively heated and partly ionized preshock gas. In this model far-IR radiation is produced by UV-heated dust grains in a preshock layer of gas, photoionized by a radiative precursor preceding the shock front.

4. Draine & Woods (1990) have considered X-ray irradiation of molecular clouds. The X-rays create energetic photoelectrons in the molecular gas that is collisionally heated to a few thousand kelvins and produces strong vibrational emission from collisionally excited H_2. Draine & Woods (1990) apply this model to NGC 6240 and conclude that fast shocks or SNRs can produce the required X-ray flux.

The observed H_2/Brγ ratio of about 45 for NGC 6240 provides an important constraint on the J-shock models (Hollenbach & McKee 1989). Inspection of the J-shock model spectra reveals that the observed H_2/Brγ ratio can only be produced in shocks with $v_s \lesssim 45$ km s^{-1} for $n_0 = 10^3$–10^5 cm^{-3}, or with $v_s \lesssim 35$ km s^{-1} for $n_0 = 10^6$ cm^{-3}. This constraint is very important, since it limits the maximum far-IR continuum surface brightness from the shock to about 0.3 ergs s^{-1} cm^{-2} sr^{-1} (this value is attained for $n_0 = 10^6$ cm^{-3}; for lower densities much less far-IR emission is produced; see Fig. 9 of Hollenbach & McKee 1989). The ratio of H_2 $v = 1 \rightarrow 0$ $S(1)$ line flux to far-IR flux in this model is about 0.001, so that a maximum far-IR luminosity of about 10^{11} $L_\odot$ can be produced in this shock. This value is deficient with respect to the observed far-IR luminosity by a factor of 6. This result indicates that if J-shocks give rise to the observed H_2 emission, they probably cannot produce the observed far-IR emission.

In the C-shock models published by Draine et al. (1983) no Brγ emission is produced, since any significant ionization would immediately turn the shock into a J-shock. Hence the H_2/Brγ ratio does not constrain these models. However, in this case the H_2 $v = 1 \rightarrow 0$ $S(1)$ to H_2 $v = 2 \rightarrow 1$ $S(1)$ line ratio obtained by LHC can be used as a constraint. Using Table 3 from LHC, and equation (65) and Figures 7–9 from Draine et al. (1983), it is concluded that the observed H_2 spectrum implies $v_s \approx 20$ km s^{-1} for $n_0 = 10^2$ cm^{-3}, $v_s \approx 40$ km s^{-1} for $n_0 = 10^4$ cm^{-3}, and $v_s \approx 30$ km s^{-1} for $n_0 = 10^6$ cm^{-3}. C-shocks with these parameters can produce the observed H_2 vibrational line emission from NGC 6240, but not the observed far-IR continuum emission, since, as was noted above, C-shocks produce very little far-IR continuum emission.

Next the mechanism proposed by Harwit et al. (1987), in which the H_2 emission is produced in partially ionized preshock gas, radiatively heated by the photoionizing precursor of the shock front, is considered. Harwit et al. (1987) estimate that typically 1.5×10^{-2} ergs s^{-1} cm^{-2} sr^{-1} can be emitted in the near-IR H_2 lines by this mechanism, about 1% of which comes out in the $v = 1 \rightarrow 0$ $S(1)$ line. The resulting surface brightness in this line is comparable to the surface brightness from C-shocks (Draine et al. 1983), and therefore this mechanism is at first sight a plausible explanation for the H_2 emission. However, the Harwit et al. (1987) model also produces large amounts of ionized gas, and will therefore in the case of NGC 6240 have difficulties in producing the large H_2/Brγ ratio. In order to quantify this problem, we note that the collision velocity is at least 150 km s^{-1} (the radial velocity difference of the two nuclei as measured by Fried & Ulrich 1985). Furthermore, the observed thermal population of the H_2 $v = 2$ level requires a density of approximately 10^5 cm^{-3} (Sternberg & Dalgarno 1989) in the medium emitting the H_2 vibrational lines, which in the Harwit et al. (1987) model is the preshock medium. However, a $v_s = 150$ km s^{-1} shock in a medium with a preshock density of 10^5 cm^{-3} produces a Brγ surface brightness of $\sim 3 \times 10^{-3}$ ergs s^{-1} cm^{-2} sr^{-1} (Hollenbach & McKee 1989), so that the H_2/Brγ ratio predicted for NGC 6240 by the Harwit et al. (1987) model is ~ 0.05, three orders of magnitude smaller than the observed value of 45. This argument rules out the Harwit et al. (1987) model for the H_2 emission from NGC 6240.

Finally, H_2 excitation due to X-rays, as proposed by Draine & Woods (1990), is considered. These authors argue that the H_2 emission from NGC 6240 can be produced by $\sim 10^{10}$ $L_\odot$ of soft X-rays absorbed in molecular clouds with $n \sim 10^5$ cm^{-3} (in order to thermalize the $v = 2$ level; see above). The X-ray energy deposited per unit volume in the initially neutral gas is $\gamma n_{\rm H}$, where $n_{\rm H}$ is the density of hydrogen nuclei. Using $\gamma = 2 \times 10^{-19}$ ergs s^{-1}, following Draine & Woods (1990), and a penetration column density for the X-rays of $\sim 5 \times 10^{19}$ cm^{-2}, an H_2 $v = 1 \rightarrow 0$ $S(1)$ surface brightness of $\sim 4 \times 10^{-3}$ ergs s^{-1} cm^{-2} sr^{-1} is produced, assuming that about 0.5% of the absorbed energy is emitted in this line (Draine & Woods 1990). Although this surface brightness is comparable to that produced in C-shocks (see above), several problems occur when this model is applied to NGC 6240. In the first place, excitation by X-rays produced by SNRs (as favored by Draine & Woods) is unlikely, since a supernova rate of ~ 7 yr^{-1} would be required (Draine & Woods 1991), while the actual SN rate in NGC 6240 implied by the radio emission is only 2 yr^{-1} (as will be shown in § 4.2.2). More important, as noted above, in this case the H_2 emission would be expected to follow the stellar light, contrary to what is observed. Excitation by X-rays from an obscured AGN has a morphological problem as well, since it is not clear how the observed extended H_2 emission could be produced by a localized source of excitation, which moreover would not be located at the peak of the H_2 emission but in one (or both) of the nuclei of NGC 6240. In addition, the AGN model fails on energetic grounds, as is shown by the following argument. Rieke (1988) has found a 2 σ upper limit of 10^9 $L_\odot$ for the hard (2–10 keV) X-ray luminosity of NGC 6240 from *HEAO* A-1 data. Since typically $A_{2-10\,\rm keV} \sim 0.1 A_{2.2\,\mu\rm m}$ (Rieke 1988), and since furthermore the soft (0.5–3.5 keV) X-ray flux from Seyfert 1 nuclei roughly equals the hard X-ray flux, this luminosity limit may be used as an order-of-magnitude estimate for the maximum *intrinsic soft X-ray* luminosity of an obscured AGN in NGC 6240. It is then concluded that if an AGN is present in NGC 6240 (which is not ruled out by this argument), its soft X-ray luminosity is an order of magnitude too low to account for the H_2 emission via the Draine & Woods (1990) model. Estimating the soft X-ray flux from the Brγ flux or 6 cm continuum flux density using the empirical relations found by Ward (1988) and Forbes et al. (1992) for starburst galaxies likewise results in soft X-ray luminosities that are too low. A more promising possibility (from a mor-

phological point of view) is excitation by X-rays produced in fast shocks resulting from the collision of the two interstellar media. As shown by Draine & Woods (1990), this mechanism is energetically feasible. However, in this case the high $H_2/Br\gamma$ ratio cannot be explained. As noted above, a shock with $v_s = 150$ km s^{-1} (slower shocks do not produce enough soft X-rays), propagating in the medium that also emits the H_2 lines, so that the preshock density is $\sim 10^5$ cm^{-3} (see above), produces a Brγ surface brightness of $\sim 3 \times 10^{-3}$ ergs s^{-1} cm^{-2} sr^{-1}, so that the $H_2/Br\gamma$ ratio would be about 1.3, more than 30 times lower than the observed value of 45. Recombination line emission from the postshock region is much weaker if the shock propagates in a low-density (e.g., intercloud) medium and the X-rays produced by the shock irradiate denser molecular clouds. However, in this case bright Brγ emission will be generated by collisionally ionized gas at the cloud surfaces. As shown by Draine & Woods (1990), the X-ray–excited H_2 layer only survives for about 10 yr before collisional dissociation and ionization begin to dominate. When molecular line cooling ceases, the resulting layer of ionized gas is quickly heated to about 10^4 K (Lepp & McCray 1983; Draine & Woods 1990). Using an electron density $n_e \sim 10^5$ cm^{-3} and the soft X-ray penetration column density given above, an emission measure of $\sim 2 \times 10^6$ pc cm^{-6} is found for the ionized layer, and the emerging Brγ surface brightness will be $\sim 2 \times 10^{-3}$ ergs s^{-1} cm^{-2} sr^{-1}. The resulting $H_2/Br\gamma$ ratio of about 2 may be increased by about a factor of 2 by noting that the H_2 line–emitting layer survives for about 10 yr, while the Brγ-emitting layer is expected to dissolve into the ambient medium after about 5 yr (Draine & Woods 1990), but this increase is not enough to reproduce the observed $H_2/Br\gamma$ ratio of 45. It is thus concluded that none of the various mechanisms considered can produce the X-rays required by the Draine & Woods (1990) model for the H_2 emission from NGC 6240 in a manner consistent with the available data. Hence X-ray excitation as the origin of the observed H_2 emission is unlikely.

These considerations lead to the following important conclusions. The H_2 emission from NGC 6240 is produced in C-shocks such as modeled by Draine et al. (1983), or in slow ($v_s \lesssim 40$ km s^{-1}) J-shocks as modeled by Hollenbach & McKee (1989). Since the H_2 $v = 1 \rightarrow 0$ $S(1)$ surface brightness produced by a C-shock exceeds that produced by a J-shock (with the same shock speed and preshock density) by one to two orders of magnitude, C-shocks can much more easily account for the observed intense H_2 emission from NGC 6240 and are therefore favored. The shocks producing the H_2 vibrational emission cannot account for the observed far-IR emission from NGC 6240.

4.1.2. *Relation to the Optical Line Emission*

It is interesting to compare the maximum allowed shock speed of ~ 40 km s^{-1} in the molecular gas to the relative radial motion of the nuclei of NGC 6240. Optical spectroscopy of the nuclei (Fried & Ulrich 1985) reveals a radial velocity difference of ≈ 150 km s^{-1}. Allowing for the presence of a velocity component perpendicular to the line of sight, this value serves as a lower limit to the interaction velocity of the nuclei. If it is assumed that the gas in the central regions of NGC 6240 has an isotropic velocity distribution, then the CO line width of $\simeq 320$ km s^{-1} of the main gas concentration in NGC 6240 (Wang et al. 1991) can be used as an upper limit to the interaction velocity. Thus the collision velocity must lie between about 150 and 300 km s^{-1}. Since it was concluded in § 4.1.1 that the H_2 data allow shock speeds of at most ~ 40 km s^{-1}, a mechanism must be found to produce such slow shocks if the original collision velocity is much higher.

A simple explanation can be found by considering a shock propagating in an inhomogeneous interstellar medium (ISM). If a shock propagating in a medium with mass density ρ_1 at shock speed v_1 encounters a gas layer with mass density ρ_2, the shock speed v_2 in this layer will be

$$v_2 = v_1 \sqrt{\frac{\rho_1}{\rho_2}}, \tag{1}$$

neglecting factors of order unity (Spitzer 1978, his eq. [12-39]). Hence the observed minimum collision velocity can be reconciled with the maximum shock velocity allowed by the H_2 data if the collision originally generates a fast ($v \gtrsim 150$ km s^{-1}) shock in a low-density ISM, possibly an intercloud medium or a system of diffuse low-density atomic clouds. When this shock encounters a molecular cloud, a slower shock will propagate in the denser molecular gas, commensurate with the above conclusions. As a variation on this model, it is possible that the rapid merging of the intercloud media of the colliding galaxies will lead to a pronounced pressure increase at the surfaces of the molecular clouds, leading to slow shocks moving radially inward into the clouds, as proposed by, e.g., Jog & Solomon (1992).

This scenario is in agreement with a simple argument based on the molecular cloud properties of our Galaxy. For our Galaxy the volume filling factor of giant molecular clouds (GMCs) is $f \sim 0.01$, and the typical radius of a GMC is $R \sim 30$ pc (Sanders, Scoville, & Solomon 1985). The scale height of the GMC population is $z \sim 100$ pc (Sanders, Solomon, & Scoville 1984). If two galaxies with such a cloud population collide, the mean free path of an individual cloud is $(2/3)R/f \approx 2$ kpc (for spherical clouds). Since this value exceeds the cloud scale height of the collision partners by a large factor, direct cloud-cloud collisions are very unlikely (except in the improbable case of an edge-on collision). This argument shows that the above scenario, where individual clouds are only affected by shocks propagating in a more pervasive, low-density medium, or by slow shocks generated by the overpressure of the merged intercloud media, is naturally expected in an encounter between galaxies with cloud populations similar to those in our Galaxy.

In order to test this scenario, the presence of fast shocks in a low-density medium in NGC 6240 will be investigated. Such shocks cool by the emission of fine-structure lines and recombination lines, and their presence can thus be tested by an analysis of the emission-line spectrum of NGC 6240. Indeed, many authors (e.g., Fosbury & Wall 1979; Fried & Schulz 1983; Rieke et al. 1985; Heckman et al. 1987; Kirhakos & Phillips 1989; Keel 1990) have pointed out that the optical spectrum of NGC 6240, with strong emission from neutral or low-ionization species, is not characteristic of photoionization but is a typical shock-excited LINER spectrum. In order to estimate the physical parameters implied by this spectrum, spectral-line data have been taken from Fosbury & Wall (1979), Fried & Ulrich (1985), Morris & Ward (1988), Armus et al. (1989), Kirhakos & Phillips (1989), and Keel (1990). Synthetic spectra of fast radiative shocks have been published by Dopita (1977), Shull & McKee (1979), Raymond (1979), Binette, Dopita, & Tuohy (1985), Innes, Giddings, & Falle (1987), Hartigan, Raymond, & Hartmann (1987), and Shull &

Draine (1987). For higher preshock densities ($n_0 \sim 10^3$–10^4 cm^{-3}) the J-shock models by Hollenbach & McKee (1989) may be used. Since a range of shock velocities and preshock densities probably exists in NGC 6240, it is unlikely that a single shock model can reproduce the observed spectrum. Furthermore, there is considerable scatter between the predictions of the various models listed above. Nevertheless, certain combinations of lines observed in NGC 6240 lead to similar constraints in all of these shock models. The following constraints can be derived:

1. The shock velocity must be at least 100 km s^{-1}. The line ratios [O II $\lambda\lambda$7320+7330]/Hα, [N II $\lambda\lambda$6548+6584/Hα], [Ne III λ3869]/Hβ, and [O III $\lambda\lambda$4959+5007]/[O I $\lambda\lambda$6300 +6364] would be much lower than observed if v_s were less than 100 km s^{-1}.
2. The maximum shock velocity allowed by the optical spectrum is about 200 km s^{-1}. For higher shock velocities the line ratios [O I $\lambda\lambda$6300+6364]/Hα and [S II $\lambda\lambda$6717+6731]/Hα would be much higher than observed, while [O III $\lambda\lambda$4959 +5007]/[O I $\lambda\lambda$6300+6364] would be lower than observed.
3. Heckman et al. (1990) have used the [S II] $\lambda\lambda$6717, 6731 doublet ratio to derive an electron density of $\sim$500 cm^{-3} in the central regions of NGC 6240. Standard shock models with v_s = 100–200 km s^{-1} (see above) then imply a preshock density of about 10 cm^{-3}.

It is concluded that the optical emission-line spectrum of NGC 6240 can be accounted for by radiative shocks with v_s = 100–200 km s^{-1} in a medium with $n_0 \sim 10$ cm^{-3}. This result is consistent with our suggestion that slow shocks in the dense molecular medium of NGC 6240, observed by their H_2 vibrational line emission, result from a faster shock propagating in a more tenuous medium and resulting directly from the collision of the two interstellar media.

To conclude this part of the analysis, we consider the IR continuum emission produced by the fast shock propagating in a low-density medium in NGC 6240. Wright et al. (1988) have presented a north-south 10 μm profile of NGC 6240, which shows the 10 μm emission to be concentrated within $\sim$2″. Since this size is much smaller than the extent of the Hα emission (Heckman et al. 1987; Armus et al. 1990; Keel 1990), it is unlikely that much of the IR emission is produced in the fast shock. A quantitative estimate of the expected far-IR luminosity can be made using the results of Draine (1981), who considered the collisional heating of dust grains in shock-heated gas. Using his equation (30), a maximum far-IR surface brightness of $\sim 7 \times 10^{-3}$ ergs s^{-1} cm^{-2} sr^{-1} is derived for n_0 = 100 cm^{-3} and v_s = 200 km s^{-1}. This brightness, which decreases strongly with decreasing n_0 and v_s, is a factor of 5 higher than the peak surface brightness of the H_2 $v = 1 \rightarrow 0$ $S(1)$ line. Combined with the size of the emitting region of $\sim$2″ (see above) and the measured H_2 luminosity (§ 4.1.1), it is estimated that at most $\sim 10^9\ L_\odot$ of far-IR emission can be produced by these shocks, which is completely negligible compared with the observed far-IR luminosity. Draine (1981) ignores dust heating due to the absorption of UV photons produced in the shock, which may not be a good approximation at the low densities considered here. In order to assess the effect of UV absorption, the models by Hollenbach & McKee (1989), where this effect is included, may be used. In these models a far-IR surface brightness of about 10^{-2} ergs s^{-1} cm^{-2} sr^{-1} is produced for v_s = 150 km s^{-1} and $n_0 = 10^4$ cm^{-3}, strongly decreasing with decreasing density. Comparing this brightness with that derived from the Draine (1981) model, it is concluded this mechanism cannot account for the observed far-IR emission either. In summary, neither the shock producing the H_2 emission nor the shock producing the optical line emission can account for a significant fraction of the far-IR emission from NGC 6240.

4.2. [Fe II] *Emission*

4.2.1. *Origin of the* [Fe II] *Emission*

In contrast to the H_2 emission, the [Fe II] emission from NGC 6240 is dominated by the two nuclei, as shown in Figure 2. The [Fe II] emission thus follows the optical and near-IR continuum emission, and also the nonthermal radio emission (Carral et al. 1990; Eales et al. 1990). The luminosity ratio of the two nuclei in the [Fe II] line is 1.63, the southern nucleus being the brighter one. This ratio is in good agreement with the ratio of the 6 cm radio continuum fluxes of 1.75 (Eales et al. 1990). Furthermore, Carral et al. (1990) note the presence of a diffuse radio continuum component around the two nuclei, containing about 40% of the total radio flux at 2 cm. This fraction is identical to the fraction of the [Fe II] emission contained in a possible extended component (see § 3.2).

In order to decide what the origin of the [Fe II] emission is, we note that the ratio [Fe II]/Brγ from the nuclei of NGC 6240 is $\gtrsim$12. Since this number was calculated under the assumption that the entire Brγ flux of NGC 6240 originates in the nuclei, and ignores any differential reddening between the [Fe II] and Brγ lines, this value is actually a lower limit. Such high ratios of [Fe II]/Brγ are only observed in SNRs (e.g., Graham, Wright, & Longmore 1987, 1990; Oliva, Moorwood, & Danziger 1989, 1990). The bright [Fe II] emission from these objects is due to a combination of two mechanisms:

1. In shocks most of the available gas-phase iron is singly ionized, because Fe^{2+} is immediately converted into Fe^+ by charge exchange with atomic hydrogen, which is extremely rapid (Neufeld & Dalgarno 1987). In contrast, charge exchange between Fe^+ and atomic hydrogen is endothermic by 5.7 eV, and therefore slow at typical post shock temperatures. As a result, in fast shocks most of the gas-phase iron is maintained in the form of Fe^+. In H II regions, on the other hand, the atomic hydrogen fraction is very much lower than in shocks, so that charge transfer with atomic hydrogen does not affect the iron ionization balance. As a result, the balance of photoionization and radiative recombination maintains most of the iron in *photoionized* regions in the form of Fe^{2+}, giving rise to very low [Fe II]/Brγ ratios. Indeed, the measured value of [Fe II]/Brγ in the Orion Nebula is 0.06 (Lowe, Moorhead, & Wehlau 1979; see also Greenhouse et al. 1991). These considerations are analyzed in more detail by Blietz et al. (1993).
2. In fast ($v_s \gtrsim 100$ km s^{-1}) shocks the gas-phase abundance of iron is enhanced by the destruction of dust grains by thermal sputtering (e.g., Seab 1987; Draine 1990). In the general ISM gas-phase iron is depleted by a factor of about 50 (e.g., Phillips, Gondhalekar, & Pettini 1982; Harris, Gry, & Bromage 1984; Van Steenberg & Shull 1988; De Boer, Jura, & Shull 1987) with respect to the solar abundance of 2.5×10^{-5} (Cameron 1973). Theoretical calculations show that thermal sputtering of refractory grains in fast shocks may enhance the gas-phase iron abundance with a factor of up to 30 with respect to its normal value (Seab & Shull 1983; McKee et al. 1987).

Because of its high gas-phase abundance, the low ionization potential (7.9 eV) of neutral iron, and the large number of

energy levels of Fe^+ at $E/k \sim 10^4$ K, the typical temperature of the cooling post-shock gas, Fe^+ is a major coolant for fast shocks (cf. partial term diagrams presented by Allen, Jones, & Hyland 1985, Oliva et al. 1990, and Haas et al. 1990). Published shock models including grain processing indicate that bright [Fe II] lines are emitted for $v_s \gtrsim 100$ km s^{-1} (McKee, Chernoff, & Hollenbach 1984; Shull & Draine 1987). In these models Fe^+ is excited by collisions with electrons in the cooling postshock gas.

An alternative excitation model has been proposed by Graham et al. (1990). In order to account for the observed [Fe II] emission from the Crab Nebula, these authors propose that the UV and X-ray emission from the SNR produces an extended zone of warm gas, where hydrogen is predominantly neutral and iron singly ionized. Graham et al. (1990) suggest that this mechanism may also account for the bright [Fe II] emission from AGNs.

The high [Fe II]/Brγ ratio thus strongly suggests that the [Fe II] emission from the nuclei of NGC 6240 is produced by SNRs. This interpretation also provides a natural explanation for the observed correlation of the [Fe II] flux with nonthermal radio flux density observed in NGC 6240. The relation of [Fe II] and radio emission will be discussed in the next section.

4.2.2. *Comparison of* [Fe II] *and Radio Emission*

In order to enable a quantitative comparison between the [Fe II] and radio emission, first the extinction toward the [Fe II] line–emitting medium is derived. This extinction follows directly from the observed [Fe II] 1.257 μm/1.644 μm ratio. The 1.257 μm line ($a^4D_{7/2} \rightarrow a^6D_{9/2}$) arises from the same upper level as the 1.644 μm line, and the intrinsic line ratio depends only on atomic parameters. Using the parameters given by Nussbaumer & Storey (1988), the intrinsic 1.257 μm/1.644 μm line ratio is 1.36, while the observed ratio derived from our slit spectroscopy is 1.04. Using the near-IR reddening law given by Koornneef (1983), near-IR extinctions $A_K = 0.2$ mag and $A_H = 0.3$ mag are derived. At these small extinctions, it is irrelevant whether the dust is assumed to be mixed with the emitting medium or located in front of it (cf. Thronson et al. 1990). We thus derive an intrinsic [Fe II] flux from the nuclei of 1.6×10^{-13} ergs s^{-1} cm^{-2}, corresponding to an intrinsic luminosity of 4.9×10^7 $L_\odot$ in this line.

The radio synchrotron emission from the nuclei of NGC 6240 may be used to obtain a supernova rate ν_{SN} (e.g., Völk 1989) that can be compared with the [Fe II] fluxes. The 6 cm fluxes by Eales et al. (1990) will be used, since these are obtained at an angular resolution similar to the seeing of the present near-IR observations. The formula

$$\nu_{SN} = 3.3 \times 10^{-6} S_{6\ cm} D^2 \qquad (2)$$

is used, where ν_{SN} is in yr^{-1}, $S_{6\ cm}$ is the nonthermal 6 cm flux in mJy, and D is the distance in Mpc. The numerical factor in equation (2) is based on the radio flux, supernova rate, and pulsar birthrate of our Galaxy (Condon & Yin 1990) and correctly accounts for the fact that the electrons accelerated by the SNR shocks radiate most of their energy after the individual SNRs have disappeared (as pointed out by, e.g., Ilovaisky & Lequeux 1972). From equation (2) the values $\nu_{SN} = 1.4$ yr^{-1} and $\nu_{SN} = 0.7$ yr^{-1} are obtained for the southern and northern nucleus, respectively. Interestingly, the total supernova rate of 2.1 yr^{-1} agrees well with the value of 1.8 yr^{-1} derived by Heckman et al. (1990) using a completely different method, examining the observed radial gas pressure profile in the context of the superwind model. In order to relate the derived values to the [Fe II] fluxes, we note that the total energy radiated by one SNR in the post-Sedov phase, when the SNR shock has become radiative and the hot postshock gas cools by line emission, is $0.651E_0$ (Draine & Woods 1991), where E_0 is the energy released in the supernova explosion. Since a strong cooling line in a radiative shock typically accounts for $\sim 1\%$ of the energy radiated away, the total energy radiated in the [Fe II] 1.64 μm line by one SNR can be written as $6.51 \times 10^{-3} \eta E_0$, where η is of order unity. Let this energy be emitted over a period of $t_{[Fe\ II]}$ yr; then the average [Fe II] 1.64 μm luminosity of one SNR over this period is $6.51 \times 10^{-3} \eta E_0 / t_{[Fe\ II]}$ ergs yr^{-1}. Furthermore, there are then at any moment $\nu_{SN} t_{[Fe\ II]}$ SNRs emitting in the 1.64 μm [Fe II] line, so that the expression

$$L_{[Fe\ II]}/L_\odot = 5.4 \times 10^7 \eta \nu_{SN} (E_0/10^{51}\ \text{ergs}) \qquad (3)$$

is obtained for the intrinsic [Fe II] 1.64 μm luminosity from a starburst. With the intrinsic $L_{[Fe\ II]} = 4.9 \times 10^7$ $L_\odot$ for the two nuclei together, and the ν_{SN} values derived above, $\eta = 0.9$, in agreement with the assumption that the [Fe II] 1.64 μm line is a major coolant for radiative SNR shocks.

The average [Fe II] 1.64 μm luminosity of an individual radiative SNR is $4.9 \times 10^7/(\nu_{SN} t_{[Fe\ II]})$ $L_\odot$. An estimate for $t_{[Fe\ II]}$ can be obtained by comparing the collective volume of the SNRs created in the starburst to the total volume of the nuclei. High-resolution radio images (Carral et al. 1990; Eales et al. 1990) show that the radio nuclei of NGC 6240 have diameters of $\sim 0\farcs5$ or less ($\lesssim 250$ pc), corresponding to a total volume of $\sim 2 \times 10^7$ pc^3 for the two nuclei together. Moorwood & Oliva (1988) have used their observed upper limit on the [Fe II]1.600 μm/1.644 μm line ratio to derive an upper limit of $n_e < 5 \times 10^3$ cm^{-3} for the postshock electron density. For a reasonable compression in a radiative shock (e.g., Hollenbach & McKee 1989) the preshock density can then be estimated to be ~ 30–50 cm^{-3}. The corresponding radius of an individual SNR at the beginning of the radiative phase is ~ 6 pc (Draine & Woods 1991). The two nuclei can contain at most $\sim 2 \times 10^4$ SNRs of this size, so that the individual SNRs must begin to merge after about 10^4 yr. Using this value for the lifetime of a typical bright [Fe II] emitting SNR in the nuclei of NGC 6240 yields an average [Fe II] 1.64 μm luminosity of 2300 $L_\odot$ for such SNRs. Obviously, there is a considerable uncertainty in this value, but it is a useful order-of-magnitude estimate. The value obtained is high compared with typical $L_{[Fe\ II]}$ values observed in Galactic and LMC SNRs, where $L_{[Fe\ II]} \lesssim 720$ $L_\odot$ has been observed (Oliva et al. 1989), but is similar to the [Fe II] 1.64 μm luminosities found for SNRs in the starburst galaxies M82 (Greenhouse et al. 1991) and NGC 253 (Forbes et al. 1993).

The gas-phase iron abundance can be estimated from the observed [Fe II]/Brγ ratio. It is easily verified that electron impact dominates the excitation of the relevant [Fe II] levels in fast shocks, so that the [Fe II] 1.644 μm surface brightness (in ergs s^{-1} cm^{-2} sr^{-1}) can be expressed as

$$I_{[Fe\ II]} = \frac{h\nu}{4\pi} A x \frac{n_u}{n_{Fe^+}} \frac{N_{Fe^+}}{N_H} N_e , \qquad (4)$$

where $A = 4.65 \times 10^{-3}$ s^{-1} (Nussbaumer & Storey 1988) is the Einstein coefficient for spontaneous emission in the 1.64 μm line and N_e is the column density of electrons in cm^{-2}. The factor n_u/n_{Fe^+} is the fraction of Fe^+ ions in one of the four

fine-structure levels of the a^4D term, while x is the fraction of these in the $J = 7/2$ state. In order to evaluate equation (4), we make use of the limit $n_e < 5 \times 10^3$ cm^{-3} found by Moorwood & Oliva (1988) for the [Fe II] 1.64 μm emitting medium. Comparing this upper limit with the critical densities of the a^4D and a^4F terms (see Nussbaumer & Storey 1980, 1988), it is seen that these levels are subthermally excited, so that $n_u/n_{Fe^+} \propto n_e$. Furthermore, in this case most of the [Fe II] ions in the a^4D term will be in the lowest ($J = 7/2$) state, so that $x \approx 1$. Using $T \sim 7500$ K (a value typical for shock-excited [Fe II] emission in Galactic SNRs; Graham et al. 1987) and the atomic parameters given by Nussbaumer & Storey (1980, 1988), the expression $n_u/n_{Fe^+} \approx 6 \times 10^{-7} n_e$ is derived for subthermal excitation of the a^4D level, where the Fe^+ ion has been treated as a three-level system (a^4D, a^4F, and a^6D). Equation (4) can now be written as

$$I_{[Fe\ II]} = 8 \times 10^{-4} \frac{N_{Fe^+}}{N_H} EM , \quad (5)$$

where EM is the usual emission measure in pc cm^{-6}. For $T \sim 7500$ K, the Brγ surface brightness is

$$I_{Br\gamma} = 1 \times 10^{-9} EM \quad (6)$$

(Hummer & Storey 1987), so that the observed [Fe II]/Brγ ratio implies $N_{Fe^+}/N_H \sim 2 \times 10^{-5}$. Thus about the total solar iron abundance must be available in the nuclei of NGC 6240 in the form of Fe^+. Since we have ignored the fact that a large fraction of the observed Brγ flux is probably due to photoionization by stars in the nuclear starburst, and not generated in the fast shocks producing the [Fe II] emission, the derived gas-phase Fe^+ abundance is in fact a lower limit. This analysis demonstrates the necessity of grain destruction to account for the high [Fe II]/Brγ ratio (cf. § 4.2.1), and thus confirms the correctness of our interpretation of the [Fe II] emission as originating in fast shocks in the nuclei of NGC 6240.

The FWHM of the [Fe II] lines of 630 km s^{-1} is significantly lower than the $\sim$1000 km s^{-1} width of Hα in this region (Heckman et al. 1990). Furthermore, the high-velocity wings that were found in the H_2 spectra (Fig. 3) are absent in the [Fe II] profile (Fig. 5). This absence suggests that little [Fe II] emission is associated with the high-velocity parts of the superwind (in contrast to the situation for H_2; see § 4.1), most likely as a result of the low density in the superwind, which leads to a very subthermal population of the a^4D levels. We note that the slow ($\sim$40 km s^{-1}) shocks producing the H_2 emission do not produce any [Fe II] emission. The fast shocks generating the slower shocks (as argued in § 4.1.2) propagate in a low-density medium, possibly giving rise to extended low surface brightness [Fe II] emission. The presence of faint extended [Fe II] emission (too faint to be detected in Fig. 4) was suggested in § 3.2. The fact that high surface brightness [Fe II] emission is only detected from the nuclei simply reflects the fact that the shock activity peaks strongly in the nuclei, where the supernova explosions occur as shown by the radio emission. In addition, the gas density in the nuclei may be somewhat higher, leading to a less subthermal population of the a^4D levels of Fe^+ in the shocked gas. The observed width of [Fe II] lines is then the result of the high injection rate of mechanical energy into a relatively small volume of interstellar gas by multiple supernova explosions.

4.3. *NGC 6240 as a Starburst Galaxy*

The picture emerging from the above analysis of the H_2 and [Fe II] data is that the far-IR emission from NGC 6240 is produced in a nuclear starburst that also gives rise to the observed [Fe II] and nonthermal radio emission. The H_2 emission, on the other hand, is produced in a global shock resulting from the merging of two galaxies, and that also accounts for the optical emission-line ratios but does not contribute to the far-IR emission. This conclusion is consistent with the fact that NGC 6240 follows the radio–far-IR correlation for starburst galaxies.

The most common argument against the starburst model for NGC 6240 is based on the low Brγ flux (see § 1.1). This problem will now be considered. After correction for the extinction derived in § 4.2.2, the intrinsic Brγ luminosity of NGC 6240 is $\sim 3.1 \times 10^6\ L_\odot$. Making the usual assumption of dust-free, ionization-bounded photoionized regions with $T_e \sim 10^4$ K, the corresponding production rate of Lyman continuum photons is $Q = 1.0 \times 10^{54}$ s^{-1} (e.g., Osterbrock 1989). Together with the bolometric luminosity $L_{bol} = 6 \times 10^{11}\ L_\odot$ of NGC 6240, these numbers may be compared with the time-dependent starburst models described by Scoville & Soifer (1991). Using a standard initial mass function [IMF; $\psi(M) \propto M^{-\gamma}$ with $\gamma = 2.5$], these authors derive the expression

$$\frac{L_{bol}}{Q} = 1.20 \times 10^{-43} \left(\frac{m_u}{45\ M_\odot}\right)^{-1.64} \left(\frac{t_B}{10^8\ \text{yr}}\right)^{0.67} L_\odot\ \text{s} \quad (7)$$

for $m_u < 45\ M_\odot$, where m_u is the upper mass cutoff of the IMF and t_B is the starburst age. Using this equation, we conclude that the starburst in NGC 6240 is deficient in massive stars, with an upper mass cutoff $m_u \sim 25\ M_\odot$. With this value of m_u the burst age is a typical 2.5×10^8 yr. A more standard IMF with an upper mass cutoff of $45\ M_\odot$ would imply an unacceptably long "burst" age of 10^9 yr. A similar constraint can be derived from the Brγ/radio continuum luminosity ratio, using the time-independent starburst models presented by Gehrz, Sramek, & Weedman (1983). For a standard IMF ($\gamma = 2.5$ and stellar masses between 6 and 40 $M_\odot$) the observed Brγ luminosity would imply a supernova rate $\nu_{SN} = 0.2$ yr^{-1}, leading to a radio flux of only 10% of the observed value. However, if an upper mass cutoff of $25\ M_\odot$ is used, the observed Brγ and radio continuum luminosity can be reproduced by starburst models.

A deficiency in massive stars is also consistent with our nondetection of the He I 2.06 μm line, since this line is powered by the most massive O stars, which produce the helium-ionizing continuum (e.g., Geballe et al. 1984). Stars with $T_{eff} < 40{,}000$ K produce nebulae where helium is underionized compared with hydrogen (e.g., Osterbrock 1989). This value of T_{eff} corresponds to ZAMS stars with spectral type O6.5 and luminosity $1.5 \times 10^5\ L_\odot$ (Panagia 1973) and mass $34\ M_\odot$ (Maeder 1987), in agreement with the upper mass cutoff derived above. In addition, the picture described above is supported by the detection of strong [Ne II] 12.8 μm emission from the NGC 6240 nuclei (Roche et al. 1991). This line can also be produced in the fast shocks traced by the [Fe II] 1.64 μm emission, but after correction for extinction the intrinsic [Ne II] 12.8 μm/[Fe II] 1.64 μm ratio is about 9, while the ratio predicted by shock models is 0.5–0.75 (Shull & Draine 1987). Therefore, the observed [Ne II] 12.8 μm flux must be dominated by photoionization. The ionization potentials of neutral and singly ionized neon are such that stars with spectral types between B1 and O7 produce the highest Ne^+ abundance in the ionized gas (De Vries 1984). The corresponding mass range is 10–30 $M_\odot$, again consistent with the upper mass cutoff derived above. The flux of ionizing photons estimated by Roche et al. (1991) from the [Ne II] 12.8 μm luminosity agrees within a

factor of 2 with the ionizing photon flux required to produce the Brγ emission.

If the star formation rate in the nuclei of NGC 6240 is allowed to decrease with time, a nonstandard IMF need not be invoked. Since a starburst is a transient phenomenon by definition, this explanation is quite natural. Moreover, a starburst can extinguish itself even before the gas reservoir is exhausted, by blowing away the gas. As shown in § 4.2.2, most of the volume of the nuclei of NGC 6240 will be occupied by hot ($\sim 10^6$ K) SNR gas. This hot medium will most likely break out of the nucleus, giving rise to a superwind that will create an extended halo of ionized gas (Chevalier & Clegg 1985). As noted above, narrow-band Hα + [N II] images (Heckman et al. 1987; Armus et al. 1990) and spectroscopy (Heckman et al. 1990) provide compelling evidence for the presence of such a superwind in NGC 6240. The postshock electron density in the nuclei of NGC 6240 is $n_e \sim 500$ cm^{-3} (Heckman et al. 1990), implying preshock densities that are much lower than expected in a medium with a substantial GMC population. These low densities may be interpreted as an indication that indeed a large fraction of the molecular medium has been removed from the nuclei of NGC 6240. The fact that the H_2 emission does not show the two nuclei is consistent with a relative absence of molecular gas in the nuclei. Likewise, the low 320 km s^{-1} FWHM of the ^{12}CO $J = 1 \rightarrow 0$ line (Wang et al. 1991), compared with the FWHM of 630 km s^{-1} of the nuclear [Fe II] line, indicates that the bulk of the molecular gas is located in relatively undisturbed (extranuclear) regions and not in the nuclei themselves. Finally, there is independent observational evidence that the relativistic electrons can escape from the nuclei of NGC 6240, giving rise to a diffuse "plume" of nonthermal radio emission (cf. radio images by Condon et al. 1982 and Antonucci 1985). We therefore suggest that the starburst in the nuclei of NGC 6240 has created a superwind that has removed a substantial fraction of the molecular medium from these two nuclei, which has led to a decreasing star formation rate in these nuclei. The detection of high-velocity H_2, most likely entrained in the superwind (see § 4.1), is direct evidence for the expulsion of molecular material from the central regions, confirming our interpretation. The same model has been applied to other fading starbursts by Rieke, Lebofsky, & Walker (1988).

As an alternative to a fading starburst to account for the low Brγ luminosity compared with the bolometric luminosity, it is possible that an AGN in NGC 6240 contributes substantially to the observed bolometric luminosity. If this AGN also contributes to the observed radio flux, the supernova rate has been overestimated, and the high radio/Brγ ratio noted above is not suprising. However, in order to make the Brγ luminosity agree with the radio emission in this model, 90% of the observed radio flux must be produced by an AGN, as shown above. Since neither of the two nuclei accounts for 90% of the radio emission, *both* nuclei must in this case possess a radio-loud AGN. While this is in principle possible, several arguments indicate otherwise:

1. If AGNs were present in NGC 6240, the optical spectrum would be that of a Seyfert galaxy, showing a range of excitation stages, as expected from a photoionized narrow-line region (NLR). Instead, the optical spectrum of NGC 6240 is a typical *shock-excited* LINER spectrum (Kirhakos & Phillips 1989), dominated by low-excitation lines of neutral and low-ionization species.

2. If only 10% of the radio flux of NGC 6240 were due to SNRs, NGC 6240 would not obey the radio–far-IR correlation, except in the very unlikely case that starburst and AGNs would conspire to produce radio and far-IR emission in the same proportions.

3. The deep CO overtone absorption bands at 2.3 μm (LHC) indicate the presence of a large population of red supergiants in the nuclei of NGC 6240. A nuclear starburst naturally accounts for this phenomenon, but in the AGN model an explanation is lacking.

4. The absence of the [Si VI] 1.96 μm line in the spectrum shown in Figure 3*b* is consistent with the absence of an AGN in NGC 6240 (cf. § 3.3).

Based on these arguments, the possibility of obscured AGNs as the main source of radio and far-IR emission in NGC 6240 is dismissed.

It is thus concluded that a starburst decreasing in strength can best account for the data. The resulting deficiency in high-mass ($M \gtrsim 25\ M_\odot$) stars accounts for the low Brγ luminosity. Since the supernova rate is dominated by stars of $M \sim 8\ M_\odot$, the [Fe II] 1.64 μm luminosity is not affected by the deficiency in high-mass stars. Thus this model also provides an explanation for the high [Fe II]/Brγ ratio. As argued above, the decreasing strength of the starburst in the nuclei of NGC 6240 is probably due to a "superwind" resulting from the intense supernova activity in the starburst region, which may have removed a substantial fraction of the molecular material from the nuclei of NGC 6240, as confirmed by the detection of high-velocity H_2 emission from material entrained in the superwind.

5. CONCLUSIONS

High-resolution ($\lesssim 1''$) images of H_2 $v = 1 \rightarrow 0$ $S(1)$ and [Fe II] 1.64 μm emission in the luminous IR galaxy NGC 6240 have been presented, together with velocity-resolved spectra of these lines. Combined with the existing body of data on NGC 6240, these data have enabled the construction of a model for the phenomena observed in this system. The following conclusions have been obtained:

1. The luminous near-IR H_2 emission observed near the nuclei of NGC 6240 is generated in a shock resulting from the merging or collision of two gas-rich disk galaxies. Support for this model comes from the observed H_2 morphology, which shows a peak located *between* the remnant nuclei of the merging galaxies, as shown in Figure 2. The total lack of morphological correspondence between the H_2 emission and the stellar light rules out any excitation mechanism directly related to stars (e.g., outflows in star-forming regions, SNR shocks, X-ray irradiation by SNRs, UV pumping) for the H_2 emission.

2. High-velocity wings of the H_2 line profile, which has a FWZI of 1600 km s^{-1}, show in addition the presence of shocked H_2 at high velocities. Based on a general morphological similarity between the H_2 emission in the fainter outer regions of the emitting area and the Hα emission, and on the large Hα line width in this area, it is concluded that the high-velocity H_2 emission originates in material entrained in and shocked by a "superwind" created in a nuclear starburst, the presence of which has been inferred from optical imaging spectroscopy.

3. From an analysis of the H_2 luminosity and a comparison with near-IR recombination line strengths, it is concluded that the H_2 emission is produced in C-type shocks with velocities of

at most ~ 40 km s^{-1}. In contrast, the relative radial velocity of the two nuclei is ~ 150 km s^{-1}, while the optical emission line spectrum is characteristic for radiative shocks with velocities from 100 to 200 km s^{-1} in a low-density ($n \sim 10$ cm^{-3}) medium. It is concluded that the galaxy collision first generated a fast shock in a low-density medium in NGC 6240, possibly an intercloud medium or a system of diffuse atomic clouds. When this shock encounters a density enhancement (i.e., a molecular cloud), a corresponding decrease in shock velocity results, leading to the slow shocks generating the observed H_2 emission. Direct cloud-cloud collisions do not occur, owing to the low volume filling factor of molecular clouds.

4. In contrast to the H_2 emission, the [Fe II] emission closely follows the stellar light and radio continuum emission from the nuclei of NGC 6240. Based on this morphology and the high [Fe II]/Brγ ratio, it is concluded that the [Fe II] emission originates in fast shocks produced by SNRs resulting from a starburst in the nuclei of NGC 6240. The [Fe II]/Brγ ratio implies a gas-phase abundance of Fe^+ in the nuclei of NGC 6240 equal to the total solar iron abundance. This high abundance can be explained by the destruction of refractory grains in fast shocks, thus confirming the interpretation of the [Fe II] emission in terms of fast shocks.

5. The total supernova rate in NGC 6240 is estimated to be ~ 2 yr^{-1} based on the nonthermal radio continuum emission. The average [Fe II] 1.64 μm luminosity of radiative SNRs in NGC 6240 is $\sim 2300\ L_\odot$. This value is higher than luminosities found for Galactic or LMC SNRs, but in agreement with values found in the starburst galaxies M82 and NGC 253.

6. The low Brγ flux from NGC 6240 indicates that the nuclei are deficient in stars more massive than about 25 $M_\odot$. This upper mass cutoff is consistent with the nondetection of the He I 2.06 μm line, which is powered by more massive stars, while the [Ne II] 12.8 μm line, powered mainly by 10–30 $M_\odot$ stars, *is* detected. The deficiency in high-mass stars is most easily explained by a starburst decreasing in strength. It is suggested that this decrease is due to the expulsion of a substantial fraction of the molecular cloud population from the nuclei of NGC 6240 by a "superwind" resulting from the intense supernova activity. The presence of high-velocity H_2 entrained in this superwind (see above) provides support for this hypothesis.

7. There is no indication for the presence of an AGN in NGC 6240.

It is a pleasure to thank the staff of the William Herschel Telescope, in particular Hans Slingerland, for their help in getting FAST on the WHT. We also thank Valentin Rotaciuc and Murray Cameron for their help with the observations, Amiel Sternberg for pointing out the importance of charge exchange for the ionization balance of iron, and Nick Scoville and the referee, Tim Heckman, for useful comments. D. A. F. acknowledges financial support from an Isaac Newton Studentship. The William Herschel Telescope is operated on the island of La Palma by the Royal Greenwich Observatory in the Spanish Observatorio del Roque de los Muchachos of the Instituto de Astrofisica de Canarias.

REFERENCES

Aitken, D. K., Roche, P. F., & Phillips, M. M. 1981, MNRAS, 196, 101P
Allamandola, L. J., Tielens, A. G. G. M., & Barker, J. B. 1985, ApJ, 290, L25
Allen, D. A., Jones, T. J., & Hyland, A. R. 1985, ApJ, 291, 280
Allen, D. A., Roche, P. F., & Norris, R. P. 1985, MNRAS, 213, 67P
Antonucci, R. R. J. 1985, ApJS, 59, 499
Armus, L., Heckman, T. M., & Miley, G. K. 1987, AJ, 94, 831
———. 1989, ApJ, 347, 727
———. 1990, ApJ, 364, 471
Baker, J. G., & Menzel, D. H. 1938, ApJ, 88, 52
Beck, S. C., Turner, J. L., & Ho, P. T. P. 1986, ApJ, 309, 70
Binette, L., Dopita, M. A., & Tuohy, I. R. 1985, ApJ, 297, 476
Blietz, M., et al. 1993, in preparation
Cameron, A. G. W. 1973, Space Sci. Rev., 15, 121
Carral, P., Turner, J. L., & Ho, P. T. P. 1990, ApJ, 362, 434
Chevalier, R. A., & Clegg, A. W. 1985, Nature, 317, 44
Condon, J. J., & Broderick, J. J. 1986, AJ, 92, 94
———. 1988, AJ, 96, 30
Condon, J. J., Condon, M. E., Gisler, G., & Puschell, J. J. 1982, ApJ, 252, 102
Condon, J. J., Huang, Z.-P., Yin, Q. F., & Thuan, T. X. 1991, ApJ, 378, 65
Condon, J. J., & Yin, Q. F. 1990, ApJ, 357, 97
De Boer, K. S., Jura, M. A., & Shull, M. J. 1987, in Exploring the Universe with the *IUE* Satellite, ed. Y. Kondo, W. Wamsteker, A. Boggess, M. Grewing, C. de Jager, A. L. Lane, J. L. Linsky, & R. Wilson (Dordrecht: Reidel), 485
De Jong, T., Klein, U., Wielebinski, R., & Wunderlich, E. 1985, A&A, 147, L6
DePoy, D. L., Becklin, E. E., & Wynn-Williams, C. G. 1986, ApJ, 307, 116
De Vries, J. S. 1984, Ph.D. thesis, Univ. Groningen
Dopita, M. A. 1977, ApJS, 33, 437
Draine, B. T. 1980, ApJ, 241, 1021
———. 1981, ApJ, 245, 880
———. 1990, in Evolution of Interstellar Dust and Related Topics, International School of Physics Enrico Fermi, Course 101, ed. A. Bonetti, J. M. Greenberg, & S. Aiello (Amsterdam: North-Holland), 103
Draine, B. T., Roberge, W. G., & Dalgarno, A. 1983, ApJ, 264, 485
Draine, B. T., & Woods, D. T. 1990, ApJ, 363, 464
———. 1991, ApJ, 383, 621
Dressel, L. L. 1988, ApJ, 329, L69
Eales, S. A., Becklin, E. E., Hodapp, K.-W., Simons, D. A., & Wynn-Williams, C. G. 1990, ApJ, 365, 478
Elston, R., & Maloney, P. 1990, ApJ, 357, 91
Fischer, J., Smith, H. A., & Glaccum, W. 1990, in Astrophysics with Infrared Arrays, ed. R. Elston (San Francisco: ASP), 63
Forbes, D. A., Ward, M. J., DePoy, D. L., Boisson, C., & Smith, M. S. 1992, MNRAS, 254, 509
Forbes, D. A., Ward, M. J., Rotaciuc, V., Blietz, M., Genzel, R., Drapatz, S., Van der Werf, P. P., & Krabbe, A. 1993, ApJ, submitted
Fosbury, R. A. E., & Wall, J. V. 1979, MNRAS, 189, 79
Fried, J. W., & Schulz, H. 1983, A&A, 118, 166
Fried, J. W., & Ulrich, H. 1985, A&A, 152, L14
Geballe, T. R., Krisciunas, K., Lee, T. J., Gatley, I., Wade, R., Duncan, W. D., Garden, R., & Becklin, E. E. 1984, ApJ, 284, 118
Gehrz, R. D., Sramek, R. A., & Weedman, D. W. 1983, ApJ, 267, 551
Graham, J. R., Wright, G. S., & Longmore, A. J. 1987, ApJ, 313, 847
———. 1990, ApJ, 352, 172
Greenhouse, M. A., Woodward, C. E., Thronson, H. A., Rudy, R. J., Rossano, G. S., Erwin, P., & Puetter, R. C. 1991, ApJ, 383, 164
Haas, M. R., Colgan, S. W. J., Erickson, E. F., Lord, S. D., Burton, M. G., & Hollenbach, D. J. 1990, ApJ, 360, 257
Harris, A. W., Gry, C., & Bromage, G. E. 1984, ApJ, 284, 157
Hartigan, P., Raymond, J. C., & Hartmann, L. 1987, ApJ, 316, 323
Harwit, M. O., Houck, J. R., Soifer, B.T., & Palumbo, G. G. C. 1987, ApJ, 315, 28
Harwitt, M. O., & Pacini, F. 1975, ApJ, 200, L127
Heckman, T. M., Armus, L., & Miley, G. K. 1987, AJ, 92, 276
———. 1990, ApJS, 74, 833
Helou, G., Soifer, B. T., & Rowan-Robinson, M. 1985, ApJ, 298, L7
Herbst, T. M., Graham, J. R., Beckwith, S., Tsutsui, K., Soifer, B. T., & Matthews, K. 1990, AJ, 99, 1773 (H+5)
Hernquist, L. 1989, Nature, 340, 687
Hollenbach, D., & McKee, C. F. 1989, ApJ, 342 306
Hummer, D. G., & Storey, P. J. 1987, MNRAS, 224, 801
Ilovaisky, S. A., & Lequeux, J. 1972, A&A, 20, 347
Innes, D. E., Giddings, J. R., & Falle, S. A. E. G. 1987, MNRAS, 224, 179
Jog, C. J., & Solomon, P. M. 1992, ApJ, 387, 152
Joseph, R. D., & Wright, G. S. 1985, MNRAS, 214, 87
Joseph, R. D., Wright, G. S., & Wade, R. 1984, Nature, 311, 132
Keel, W. C. 1990, AJ, 100, 356
Kirhados, S., & Phillips, M. M. 1989, PASP, 101, 949
Koornneef, J. 1983, A&A, 128, 94
———. 1993, ApJ, 403, 581
Krabbe, A., et al. 1993, in preparation
Larson, R. B., & Tinsley, B. M. 1978, ApJ, 219, 46
Léger, A., & Puget, J. L. 1984, A&A, 137, L5
Lepp, S., & McCray, R. 1983, ApJ, 269, 560
Lester, D. F., Harvey, P. M., & Carr, J. 1988, ApJ, 329, 641 (LHC)
Lowe, R. P., Moorhead, J. M., & Wehlau, W. H. 1979, ApJ, 228, 191
Maeder, A. 1987, A&A, 173, 247

McCarthy, P., Heckman, T. M., & van Breugel, W. J. M. 1987, AJ, 93, 264
McKee, C. F., Chernoff, D. F., & Hollenbach, D. J. 1984, in Galactic and Extragalactic Infrared Spectroscopy, ed. M. F. Kessler, & J. P. Phillips (Dordrecht: Reidel)
McKee, C. F., Hollenbach, D. J., Seab, C. G., & Tielens, A. G. G. M. 1987, ApJ, 318, 674
Moorwood, A. F. M. 1986, A&A, 166, 4
Moorwood, A. F. M., Moneti, A., & Gredel, R. 1991, Messenger, 63, 77
Moorwood, A. F. M., & Oliva, E. 1988, A&A, 203, 278
———. 1990, A&A, 239, 78
Morris, S. L., & Ward, M. J. 1988, MNRAS, 230, 639
Negroponte, J., & White, S. D. M. 1983, MNRAS, 205, 1009
Neufeld, D. A., & Dalgarno, A. 1987, Phys. Rev. A, 35, 3142
Noguchi, M. 1988, A&A, 203, 259
Nussbaumer, H., & Storey, P. J. 1980, A&A, 89, 308
———. 1988, A&A, 193, 327
Okumura, S. K., Kawabe, R., Ishiguro, M., Kasuga, T., Morita, K. I., & Ishizuki, S. 1991, in IAU Symp. 146, Dynamics of Galaxies and Their Molecular Cloud Distributions, ed. F. Combes & F. Casoli (Dordrecht: Kluwer), 425
Oliva, E., & Moorwood, A. F. M. 1990, ApJ, 348, L5
Oliva, E., Moorwood, A. F. M., & Danziger, I. J. 1989, A&A, 214, 307
———. 1990, A&A, 240, 453
Oliva, E., & Origlia, L. 1992, A&A, 254, 466
Olson, K. M., & Kwan, J. 1990, ApJ, 349, 480
Osterbrock, D. E. 1989, Astrophysics of Gaseous Nebulae and Active Galactic Nuclei (Mill Valley: University Science Books)
Panagia, N. 1963, AJ, 78, 929
Phillips, A. P., Gondhalekar, P. M., & Pettini, M. 1982, MNRAS, 200, 687
Raymond, J. C. 1979, ApJS, 39, 1
Rieke, G. H. 1988, ApJ, 331, L5
Rieke, G. H., Cutri, R. M., Black, J. H., Kailey, W. F., McAlary, C. W., Lebofsky, M. J., & Elston, R. 1985, ApJ, 290, 116
Rieke, G. H., Lebofsky, M. J., & Walker, C. E. 1988, ApJ, 325, 679
Rieke, G. H., & Low, F. J. 1972, ApJ, 175, L95
Roche, P. F., Aitken, D. K., Smith, C. H., & Ward, M. J. 1991, MNRAS, 248, 606
Rotaciuc, V. 1992, Ph.D. thesis, Univ. Munich
Sanders, D. B., & Mirabel, I. F. 1985, ApJ, 298, L31
Sanders, D. B., Scoville, N. Z., & Solomon, P. M. 1985, ApJ, 289, 373
Sanders, D. B., Soifer, B. T., Elias, J. H., Madore, B. F., Matthews, K., Neugebauer, G., & Scoville, N. Z. 1988, ApJ, 325, 74
Sanders, D. B., Solomon, N. Z., & Scoville, N. Z. 1984, ApJ, 276, 182
Scoville, N. Z., Sargent, A. I., Sanders, D. B., & Soifer, B. T. 1991, ApJ, 366, L5
Scoville, N. Z., & Soifer, B. T. 1991, in Massive Stars and Starbursts, ed. C. Leitherer, N. R. Walborn, T. M. Heckman, & C. A. Norman (Cambridge: Cambridge Univ. Press), 233
Scoville, N. Z., & Young, J. S. 1983, ApJ, 265, 148
Seab, C. G. 1987, in Interstellar Processes, ed. D. J. Hollenbach & H. A. Thronson (Dordrecht: Reidel), 491
Seab, C. G., & Shull, J. M. 1983, 275, 652
Shull, J. M., & Draine, B. T. 1987, in Interstellar Processes, ed. D. J. Hollenbach & H. A. Thronson (Dordrecht: Reidel), 283
Shull, J. M., & McKee, C. F. 1979, ApJ, 227, 131
Smith, C. H., Aitken, D. K., & Roche, P. F. 1989, MNRAS, 241, 425
Soifer, B. T., et al. 1984a, ApJ, 283, L1
Soifer, B. T., et al. 1984b, ApJ, 278, L71
Soifer, B. T., Sanders, D. B., Neugebauer, G., Danielson, G. E., Lonsdale, C. J., Madore, B. F., & Persson, S. E. 1986, ApJ, 303, L41
Solomon, P. M., Downes, D., & Radford, S. J. E. 1992, ApJ, 387, L55
Spitzer, L. 1978, Physical Processes in the Interstellar Medium (New York: Wiley)
Sternberg, A., & Dalgarno, A. 1989, ApJ, 338, 197
Tanaka, M., Hasegawa, T., & Gatley, I. 1991, ApJ, 374, 516
Telesco, C. M., & Harper, D. A. 1980, ApJ, 235, 392
Thronson, H. A., Majewski, S., Descartes, L., & Hereld, M. 1990, ApJ, 364, 456
Thronson, H. A., & Telesco, C. M. 1986, ApJ, 311, 98
Van Steenberg, M. E., & Shull, J. M. 1988, ApJ, 330, 942; erratum ApJ, 340, 624 (1989)
Völk, H. J. 1989, A&A, 218, 67
Vorontsov-Vel'yaminov, B. A. 1977, A&AS, 28, 1
Wang, Z., Scoville, N. Z., & Sanders, D. B. 1991, ApJ, 368, 112
Ward, M. J. 1988, MNRAS, 231, 1P
Wright, G. S., Joseph, R. D., & Meikle, W. P. S. 1984, Nature, 309, 430
Wright, G. S., Joseph, R. D., Robertson, N. A., James, P. A., & Meikle, W. P. S. 1988, MNRAS, 233, 1
Wrobel, J. M., & Heeschen, D. S. 1988, ApJ, 335, 677
Young, J. S., & Scoville, N. Z. 1991, ARA&A, 29, 581
Zasov, A. V., & Karachentsev, I. D. 1979, Soviet Astron. Lett., 5, 126
Zwicky, F., Herzog, E., & Wild, P. 1961, Catalogue of Galaxies and Clusters of Galaxies, Vol. 1 (Pasadena: CIT)